THE UNIVERSITY OF NEW MEXICO
HEALTH SCIENCES CENTER
COLLEGE OF PHARMACY
ALBUQUERQUE, NEW MEXICO

Correspondence Continuing Education Courses
For Nuclear Pharmacists and
Nuclear Medicine Professionals

VOLUME IX, NUMBER 3

Recent Advances in Nuclear Medicine Imaging Technology

By:

David S. Binns, ANMT
Peter MacCallum Cancer Institute
East Melbourne, Victoria
AUSTRALIA

The University of New Mexico Health Sciences Center College of Pharmacy is approved by the American Council on Pharmaceutical Education as a provider of continuing pharmaceutical education. Program No. 039-000-01-002-H04. 4.0 Contact Hours or .40 CEUs.

Approved for continuing Nuclear Pharmacy education by the Florida Pharmacy Association, Florida Program No. PSN2003-001.

PLEASE NOTE:

This lesson is worth point 4 CEUs (4 credit hours). You must complete & return two answer sheets in order to obtain full credit. Questions 1-30 must be completed on first answer sheet, questions 31-40 must be completed on the 2nd answer sheet as questions 1-10.

Recent Advances in Nuclear Medicine Imaging Technology

By:

David Binns, ANMT

RECENT ADVANCES IN NUCLEAR MEDICINE IMAGING TECHNOLOGY

STATEMENT OF OBJECTIVES

Upon completion of this material, the reader should be able to:

1. Understand the physics and selection criteria of scintillation detectors.
2. Understand the critical design issues in the development of gamma and PET cameras.
3. Discuss the relative merits of different imaging systems and how these have driven clinical acceptance.
4. Explain the technology of various gamma and PET camera innovations that have helped improve imaging performance.
5. Understand future developments in gamma and PET camera technology.

COURSE OUTLINE

INTRODUCTION

The development of radiopharmaceuticals and the evolution of nuclear medicine instrumentation often go hand in hand. There are many examples throughout the history of nuclear medicine where discoveries in one technology have driven discoveries in the other. Much of mainstream radiopharmaceutical development has focused on labeling 99m-Tc to various compounds. 99mTc wasn't selected because of its chemical properties; it was selected in part because its physical or nuclear properties elegantly matched the detector properties of the Anger gamma camera. The development of 99mTcHMPAO in the mid-1980's saw specialized fan beam collimators enter the market capable of high quality neurological SPECT. Fluorine-18 bone scanning, once in-vogue when rectilinear scanners were in general use, is know being revisited with the increasing number of PET scanners.

Nuclear medicine instrumentation is fundamentally associated with physics and to have an appreciation of this topic requires at least a minimum knowledge of these fundamentals. The physics presented in this document is by no means replete. It merely represents the basics of what is required to form a good understanding of nuclear medicine instrumentation and imaging, now and in the near future.

In the 1990s nuclear medicine continued to play an expanding role in healthcare. The growth rate in nuclear medicine services in most western countries is equal to or greater than most other diagnostic modalities and it is increasingly being recognized in many settings as a modality of choice in the cost effective clinical management of patients.

Despite this growth in technology, few recent important innovations in nuclear medicine instrumentation have been adopted by manufacturers, utilized by nuclear medicine service providers, or applied to the patient. The vast majority of nuclear medicine scans are still performed by the Anger gamma camera. The intrinsic performance specifications of the gamma camera have remained virtually unchanged over the last decade. The refining of these instruments continues but not in revolutionary terms.

There has been a remarkable but not surprising improvement in the performance of associated computing power. Processing times have been reduced, but this has been matched by increasingly complex reconstruction and display packages. Digital network technology and standardization of image formats has allowed connectivity between imaging devices, their associated work-stations, and hospital wide area networks.

Digitization of the detection system has made the gamma camera more easily calibrated and stable. Except for fan-beam collimation in neurological SPECT, there have been few new collimator designs that have reached production.

Contemporary gamma camera systems are much improved than those of a decade ago. Gantry designs are more ergonomic for patient and operator comfort, safety, and throughput. Gantries and scanning beds are now highly complex and specially engineered to perform SPECT and other studies with a high degree of precision. Body contouring (where the gantry detects the boundary of the patient's body) allows fast set-up times and reduced detector to patient distances.

Measured attenuation correction SPECT studies show promise, especially in nuclear cardiology, but still needs to gain widespread clinical acceptance. The introduction of 99mTechnetium myocardial agents and gated myocardial perfusion SPECT has reduced the problems associated with attenuation artifacts that reduce 201-Thallium specificity.

The inter-dependence of resolution and sensitivity is a major factor in gamma camera system performances. Invariably a compromise is made between the two. One simple, albeit expensive, way of making a quantum leap in system sensitivity without cost to resolution is to employ multiple detectors.[1] Increasingly dual and triple headed cameras are being employed in both SPECT and planar imaging. The increased sensitivity can be utilized to reduce statistical noise, reduce acquisition times, improve resolution, or any of these in combination.

Arguably, the most revolutionary innovation of the gamma camera in the 1990s was the development of the coincidence gamma camera allowing PET to be performed part-time. This involved significant changes to the detector electronics and logic but meant that a camera could be operated in PET or SPECT mode. Thus, the ability to perform PET was available with the purchase of an option costing in the hundreds of thousands of dollars rather than the millions needed for dedicated PET. It also meant the cost could be amortized by performing SPECT when there was limited availability of PET tracers.

Much debate has ensued about the quality of gamma camera PET versus dedicated PET. There is much clinical evaluation of gamma camera PET taking place around the world. This is a very young technology with much research and development of instrumentation taking place, particularly regarding the use of different scintillation detectors more suited to PET.

PET has had a history in medicine for almost as long as single photon nuclear medicine imaging.[2] During the 1980's and early 1990s it saw slow proliferation, primarily in neurological and myocardial research, but found few viable clinical applications. The major restraint in many instances was the high cost of PET scanning, which diluted its cost effectiveness. With the expansion of PET in oncology many centers developed more clinically based protocols and higher patient throughput, and a general change in focus away from biological, physiological, and pharmacological research. New centers opened which shared cyclotron facilities and had smaller infrastructures, which rationalized the service and reduced cost in most instances. PET scans still comprise a small percentage of total nuclear medicine services, although this percentage is growing steadily.

From a technology point of view PET still offers the potential for radical innovation. It doesn't have the restraint that collimators place on single photon imaging (Table 1), nor is it as technologically mature. This is reflected at current scientific conferences associated with imaging technology, which show an unprecedented number of papers covering new technologies associated with PET instrumentation. Some of the most important of these new directions are new scintillation detectors, depth-of-interaction and new reconstruction algorithms.

The diagnostic power of an investigation results fundamentally from its ability to contrast normal and diseased tissue. The resultant changes in radioactive distribution need to be of a suitable magnitude that can be differentiated by the imaging device.

This concept is often referred to as "signal to noise ratio" of an image, and it is the objective of Nuclear Medicine imaging equipment to maximize this value. Interestingly, it is similar to the "target to background" parameter frequently used in evaluating the performance of radiopharmaceuticals. Increasing the "signal to noise ratio" can be achieved by either improving contrast (usually by improving spatial resolution) or by decreasing noise (through increased sensitivity).[1]

It is important to appreciate the

limitations of nuclear medicine imaging devices when assessing the accuracy of a test. To do this it is necessary to understand the processes and steps involved in detecting the signal coming from the patient. In nuclear medicine, this signal is comprised of photons emitted as the result of a random event — radioactive decay.

BASIC PRINCIPLES OF DETECTION

Before Detection – Photons Through Matter

Gamma rays emitted from a decaying nucleus are monoenergetic (some isotopes have multiple but discrete photon energies). Those escaping from the patient without undergoing Compton scatter will emerge without reduction in energy. As photons travel through greater distances of body matter more will undergo collisions with the outer shell electrons of atoms comprising this matter. Following this collision the photons path will change direction and it will proceed with a reduction of energy – the greater the scatter angle the greater the loss of energy. The equation that describes the relationship between the scatter angle (q) (i.e., The angle of the change in direction following collision) and the change in photon energy is described below:

$$E_{Y2} = E_{Y1} / [\ 1 + (E_{Y1} / 511) \times (1-\cos\theta)]\ keV$$

—Where E_{Y1} is the pre-collision and E_{Y2} is the post-collision photon energies (keV)

Figure 1 shows the effect scatter has on the energies of the photons of several radionuclides. Energy windows are normally defined as a percentage of the peak so the y-axis shows the percentage energy loss at various scatter angles. Significant scatter can occur of photons at low energies, yet still be accepted by the energy window of the imaging device.

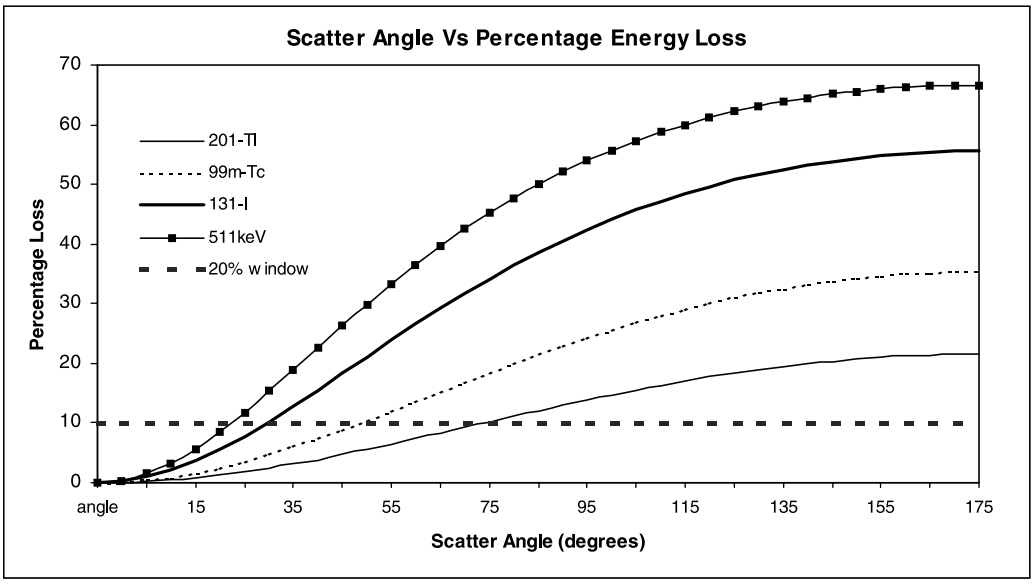

Figure 1. This graph shows the relationship between the angle of scatter of a single photon and its percentage loss in energy for 201-T1 (70 keV), 99m-Tc (140 keV), 131-I (360 keV) and 18-F (511 keV). Also shown is the 10% loss in energy that relates to a 20% (i.e., ±10%) energy window typically used for NaI(T1) detectors. Thallium-201 can undergo scatter of up to 75 degrees and still be accepted. Note that energy resolution for NaI(T1) is approximately 8% (FWHM), and hence there is a degree of inaccuracy in the measurement of a photon's energy. This means that a scattered photon that loses greater than 10% of its energy may still be included in the acceptance window.

The ability of an imaging detector to accurately discriminate the energies of scattered and unscattered photons is crucial to its performance.

Ultimately, especially in deeper structures, fewer photons will emerge unscathed. It is desirable to disregard these scattered photons. This results in reduced signal from areas where photons must travel through a greater depth of tissue to reach the detector. Indeed many photons especially those undergoing multiple Compton scattering will be stopped by the photoelectric effect. Hence, there is attenuation of signal from deeper structures.

Detector Geometry

Once photons leave the body their probability of interacting with the detector is proportional to the geometry that the detector presents to the source. In the first instance this relates to the solid angle of coverage of the detector, and secondly any collimation that may be present.

In single photon imaging the major influencing factor on the sensitivity of a detector is the collimator placed in front of it.

Collimators are a necessary but inefficient approach to obtaining positional information from photons approaching the detector. Only photons traveling perpendicular (usually) to the collimator will be allowed to pass through to the detector. No photons, even the vast majority of unscattered ones, are allowed to pass — typically as few as one in 3000 photons (0.033% for a low energy all-purpose collimator), will reach the detector. System sensitivity can be improved by designing a collimator that will admit more photons, but this is usually at the cost of resolution.

In PET scanning (assuming there is no septa) and there is a ring of detectors with a radius of 100cm and 15cm axial field of view, the geometry of a centrally place point source is around 10%. In PET scanning two of these photons need to be detected in coincidence to determine an event. However, from a geometric point of view, PET has a huge advantage over single photon imaging when it comes to the detection of events. Table 1 shows the relative efficiencies of SPECT and PET at the various steps of the detection process.

Table 1. Approximate Respective Sensitivities at Different Stages of the Detection Process for a Gamma Camera and PET Scanner.

	Gamma Camera (99m-Tc)	**PET (18-F)**
Decay		
• Relative gammas emitted	1,000,000	2,000,000
• Body absorption	250,000	1,000,000
Detector Geometry		
• Photons reaching detector	100	100,000
Detection		
• Detection of all events	75	50,000
• Energy discrimination	25	25,000
• (PET) coincidence detection		250
Events Recorded	**25**	**250**

Note that collimation causes the greatest loss of sensitivity in single photon scanners while in the PET scanner the inefficient step is the appropriate pairing of single photons into coincidences.

Scintillation Detectors

The detection of a photon emerging from the patient relies on the photon's interaction with the detector, and conversion of its electromagnetic energy into another measurable form. Almost all nuclear medicine imaging instrumentation achieves this by utilizing inorganic scintillation crystals that release light photons following absorption of the incident radiation. The light photons travel through the crystal and are subsequently detected by photo multiplier tubes (PMT), and ultimately converted to an electrical signal, the amplitude of which is proportional to the energy deposited in the crystal by the incident photon. The energies of individual photons need to be assessed to make sure that only those that have emerged unscattered and deposit all their energy in the crystal are accepted (Figure 2).

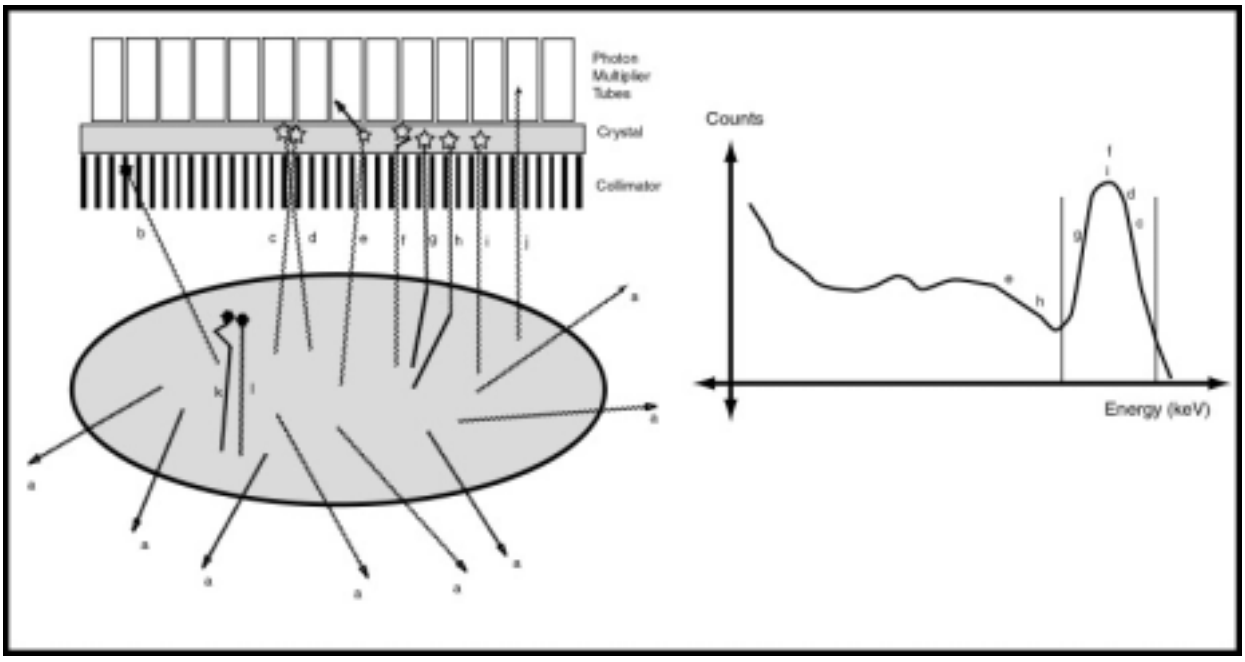

(i) Gamma camera schema **(ii) Spectrum**

Figure 2. Detection of gamma rays emitted from a patient. Only radiation traveling perpendicular to the crystal can pass through the holes of the collimator and reach the scintillation crystal (c, d, e, f, g, h, i).

- a outside detector solid angle.
- b attenuated by collimator
- c and d two photons irresolvable by detector
- e partially absorbed by detector, excluded by energy discrimination
- f scattered within crystal but totally absorbed.
- g small scatter angle – accepted by energy discrimination
- h large scatter angle – rejected by energy discrimination
- i ideal photon – no body scatter and photoelectric absorption in detector
- j no interaction with crystal
- k totally internally absorbed – multiple Compton then photoelectric absorption
- l totally internally absorbed – photoelectric absorption

(i) The energy properties of detected radiation related to their path direction and interaction with the patient, collimator, or crystal. Note that although c, d, f, and i are unscattered by the body and fully absorbed by crystal, their recorded energies vary due to relatively poor precision of the gamma camera in determining photon energy.

Detector Properties

Background

The two general types of nuclear medicine imaging are conventional nuclear medicine (planar and SPECT) and PET. These modalities have quite different requirements for detector properties and configuration.

Most conventional (i.e., single photon) nuclear medicine imaging focuses on imaging photons under 200 keV with detector count-rates under 20 k counts per second (cps). PET, conversely, images 511 keV annihilation photons, and due to the absence of collimation needs to detect these photons at system count-rates measured in the millions of counts per second.[3] PET also requires good stopping power for 511 keV photons and good energy resolution especially in systems acquiring in 3D mode.

There is also current interest in hybrid SPECT and PET systems that could perform each modality without compromising the other.

A number of physical properties can be used to evaluate scintillation detectors; these are shown below in Table 2.

Over the last two decades, detector scintillators for single photon and PET imaging have been almost exclusively developed for one modality or the other. Gamma cameras have used Sodium Iodide doped with thallium (NaI(Tl)) and Bismuth Germinate (BGO) has been used for PET. Each scintillators type has properties which makes them the most suitable for their respective imaging, but not optimal for the other. Table 3 shows the properties of a number of different detector scintillators.

Why NaI(Tl) for SPECT?

The selection of NaI(Tl) as the scintillator of choice for gamma cameras has stood the test of time. Although it has relatively poor stopping power (density and effective atomic number), it can achieve good efficiency for gamma rays with energy less than 200 keV with a 12 mm crystal thickness.

The attractive property of NaI(Tl) is its good light output per interaction (Table 3[f]). A gamma camera detector scintillator consists of a single large crystal coupled to 70-120 PMTs. When scintillation occurs the position of the emitted photon is calculated by looking at the relative electronic signal produced by all the PMTs of the detector.

Table 2. Relating desirable characteristics to physical properties of scintillation detectors.

Desirable Characteristic	Detector Property	Purpose
High detection efficiency	High atomic number and density	Improved sensitivity
Short duration of scintillation	Short light decay constant	a. High count-rate capability b. Good timing precision (hence less randoms in PET)
High detectable light output proportional to energy of absorbed gamma	High primary photon yield	Improved energy resolution
Good light transmission of appropriate wavelength to match PMT efficiency	Crystal transparency, Emission Wavelength	Improved sensitivity
Easily manufactured and processed	Availability, Strength? Hygroscopic	Reasonable cost; durability

Table 3. Properties of Various Inorganic Scintillators That Have Been Used in Gamma and PET cameras.[1,35,34,36]

a.	Density (g/cm^3)	3.67	7.13	7.40	4.54	6.71	4.88
b.	Effective Atomic Number	51	75	65	34	59	53
c.	Attenuation coefficient @ 511 keV (cm-1)	0.328	0.901	0.820	0.226	0.667	0.437
d.	Attenuation coefficient @ 140 keV (cm-1)	2.38	12.2	10	1.30		
e.	Light Decay Constant (ns)	230	300	40	70	60	0.8
f.	Relative Emission Intensity	100	15	75	120	30	12
g.	Emission Wavelength (nm)	410	480	420	440	430	220
h.	Index of Refraction	1.85	2.15	1.82	1.8	1.85	1.49
i.	Energy Resolution	8	12	12	<8	8	10
j.	Half value layer @140 keV (mm)	2.9	0.58	0.69	5.3		
k.	Half value layer @511 keV (mm)	20.8	7.6	8.3	18.0	10.4	15.8
L.	Percentage 511 keV efficiency 25 mm (12.5 mm)	56 (34)	90 (68)	87 (64)	43 (25)	81 (57)	66 (42)
m.	Manufactured cost ($US / cc)	5	15	50		25	

Sufficient photons are released by NaI(Tl) to allow this to be achieved.

When the electronic outputs of all the PMTs are added, the magnitude is proportional to the amount of light produced, which in turn is proportional to the energy absorbed by the crystal. The good light production properties of NaI give this measurement good precision, which results in good energy resolution.

In single photon imaging, the count-rates normally encountered by the detector, which is shielded by a collimator, are sufficiently low that the relatively long photon decay time doesn't cause much dead time (the minimum time it takes a detector system to correctly record two events, typically 20 microseconds).

NaI(Tl) crystals remain the optimal choice for gamma cameras doing single photon imaging. As collimator rather than crystal properties limit system resolution, there is little incentive to develop a better crystal. Much of any improvement in intrinsic resolution is negated by the effect of collimation.[1] Typically, detector (intrinsic) resolution is around 3 mm and collimator resolution 8mm. The calculation for system resolution is as follows:

$$R_{system} = \sqrt{(Rdetector2 + Rcollimator2)}$$

– Where R_{system} = resolution of system
$R_{detector}$ = resolution of detector
$R_{collimator}$ = resolution of collimator

R_{system} using the above values would be 8.5 mm. An improvement of $R_{detector}$ from

3 mm to 1 mm would result only in an improvement of R_{system} to 8.0 mm. NaI(Tl) crystals can be manufactured relatively inexpensively. They are hygroscopic and therefore need to be hermetically sealed.

Why BGO for PET?

BGO has good stopping power for 511 keV photons and achieves good sensitivity. However, it has a relatively poor light photon yield and the photons are of a wavelength not ideally suited to PMTs. This results in a relatively poor energy resolution compared to say NaI(Tl). This is one reason BGO isn't constructed into larger crystal with multiple PMTs — it doesn't have sufficient light output in such a configuration to determine the position of an event using Anger logic.

BGO PET cameras have many crystal elements (up to 20,000) arranged radially around the patient. These elements are the minimum resolving units and are typically 6 mm x 6 mm and 30 mm deep. In early models, each element was attached to a PMT, but it was difficult to pack PMTs close together. Contemporary BGO PET cameras generally use "detector modules" similar to those shown in Figure 3. Typically, 64 elements are partially cut into a single BGO block.[3] Following the absorption of a 511 keV photon by one of these elements, light is channeled along the cell until it reaches the end of the saw cuts, at which point it spreads and is observed by the four PMTs. The relative ratio of light measured by the four PMTs indicate which detector element absorbed the photon, and thus identify the position of the incident 511 keV photon.

This type of design, with small detectors, allows the camera to handle the high count-rates observed in PET. Dead time is determined by, and restricted to, the signal coming from an individual detector (or in this case a module), so with smaller detectors the measured count-rates will be lower resulting in less dead time compared to larger detectors.

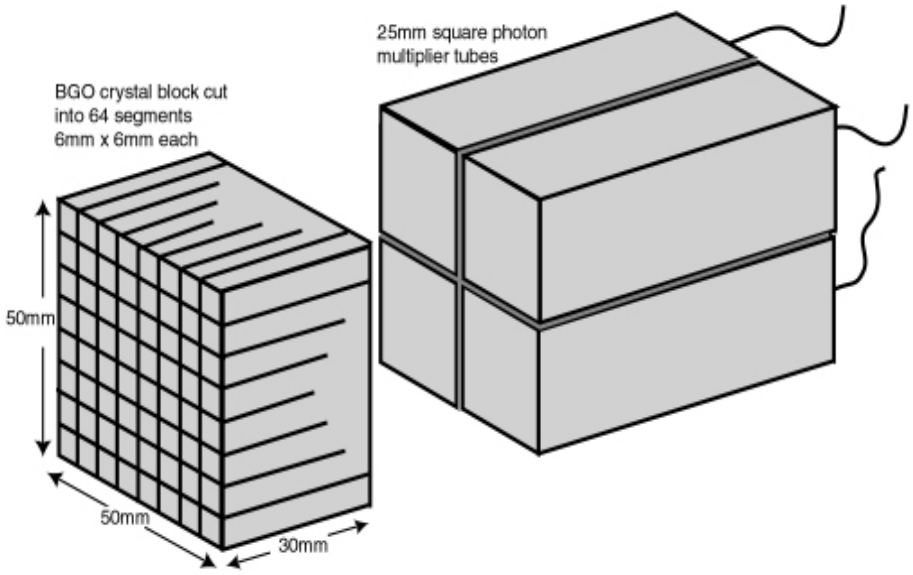

Figure 3. Diagram of a BGO PET Camera Detector Module. The module contains 8 x 8 crystal elements and four PMTs. The elements are separated by saw-cuts of varying depths. This allows the element where the event occurred to be located by comparing the ratio of light detected in each of the four PMTs.

Semi-Conductor Detectors

One of the problems associated with scintillation crystals is the inefficient way in which an incident gamma ray is recorded as an event. It requires absorption, scintillation, and conversion to an electrical signal by the PMT. The high statistical fluctuations that occur in this signal leads to poor energy resolution. As stated previously, good energy resolution enables a system to reject photons that are likely to have been scattered.

Semi-conductor detectors offer the promise of producing greater signal to noise per radiation interaction and therefore better energy resolution compared to gamma cameras.[1]

As a gamma ray passes through the semi-conductor material, it creates "electron-hole pairs" and produces ionization. The motion of "electron-hole pairs" in an applied electric field produces an electrical signal, which is proportional to the energy of the photon absorbed. The detector performance depends on the charge collection efficiency and its ability monitor leakage the gamma-induced current is much higher than the leakage current.

From a theoretical point of view, the improved signal to noise ratio of the semi-conductor detectors means a potential energy resolution of around 1%. There are problems; however, with the gamma induced electrical charges being trapped in the semi-conductor, which degrade the detector performance. The current energy resolution is approximately 3%, which should improve with further development. One of the challenges is developing sufficiently fast and complex electronics to process simultaneously the signal from large numbers of detectors.

An associated benefit of semi-conductor detectors is their smaller weight and size when compared to scintillation detectors with PMTs.

Currently the semi-conductor CdZnTe (or CZT) is showing most promise. It has a relatively high effective atomic number, resulting in good stopping power. A 7 mm thick CZT detector has equivalent stopping power to 10 mm of NaI(Tl) at 140 keV.

Semi-conductor detectors for imaging purposes will consist of one detector per image element or pixel. The size of this element will directly influence intrinsic resolution, so to be comparable in resolution with Anger gamma cameras, they will need to be approximately 3 mm x 3 mm in cross section. This would mean that, for a relatively small square shaped detector with a FOV 30 cm x 30 cm, 10^4 semi-conductors would need to be integrated.

At present, it is difficult to estimate the costs of such systems, as mass production of semi-conductor detectors and integrated circuitry will greatly improve cost efficiency. Currently there is one system produced commercially,[4] with a relatively small FOV (20 cm x 20 cm), 3 mm x 3 mm detector elements, and an impressive 250,000 cps maximum count-rate. The weight of the detector head is only 25kg and is about 8cm deep, including collimator. An equivalent Anger gamma camera would weigh approximately 150 kg and be 40 cm deep.

Tomographic Reconstruction

Filtered Back Projection (FBP)

Tomographic reconstruction takes data acquired radially and creates a transaxial slice that estimates the distribution of radioactivity within this region. FBP is the long established technique for converting the data acquired around the patient in SPECT and PET into slice or transaxial data. FBP was originally adapted from the first CT algorithms developed in the mid 1970s, and it has continued to be the only technique available from most manufacturers until the late 1990s.

During FBP, data acquired at a particular address is back projected across the image space as a line of counts whose

position is determined by the angle and address at which it was acquired. The FBP algorithm assumes that a detected event could have originated from anywhere along the line perpendicular to the collimator. Following the completion of all the back projections acquired at all angles the original point source is now represented by the superimposition of all the back projections. In Figure 4 it can be noted that there are counts deposited in the image where they shouldn't be and there is blurring of the point source. This blurring is theoretically removed by the use of a 'Ramp' Fourier filter. It does this by isolating the different frequencies that are present in the blurring and reducing them appropriately. The 'Ramp' filter is the inverse shape of the frequencies that comprise this blurring effect.

The main problem with FBP is that noise can lead to significant artifacts. In low count studies, statistical noise can lead to streaking of the data. It is particularly obvious in the low count areas surrounding hot structures and makes interpretation of these areas difficult.

FBP does not take into account the effects of attenuation, scatter and the depth dependency of collimator resolution; it assumes that data is represented by simple projection ray sums.

Iterative Methods

Iterative, or statistical, techniques achieve reconstruction by repetitively refining the reconstructed data. It does this by 'guessing' how the reconstructed data would appear to the detector and comparing it to what the acquired data actually looks like. The difference between the two is seen to be the error in the reconstructed data and appropriate modifications are made. After much iteration of approximations, the reconstructed and acquired data will (hopefully) converge.

The attraction of this technique is that the various factors that affect the signal before it reaches the detector can be modeled into the reconstruction process.[1] In theory, the effects of scatter, attenuation, and depth effect on resolution can be calculated and compared to what the detector 'sees' and be corrected.

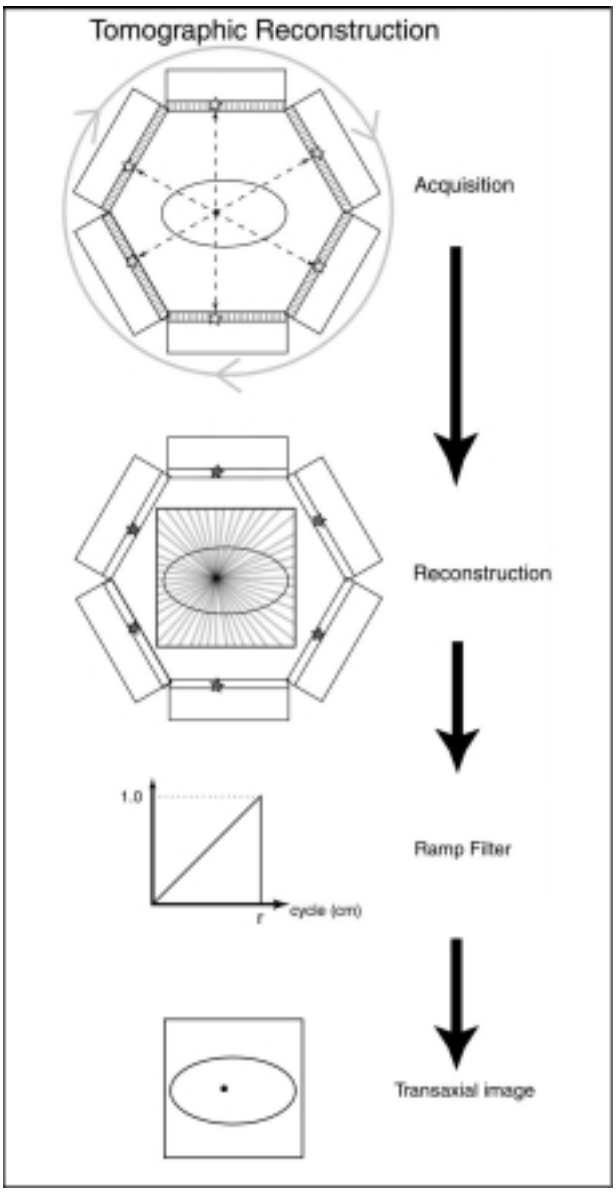

Figure 4. Acquisition and reconstruction of tomographic data into transaxial slices using FBP. The 'Ramp' Fourier filter is essential in eliminating the superimposition of ray sums created during the back-projection process.

Accelerated Methods – Ordered Subsets

The knowledge to perform iterative reconstructions in tomography has been around for some time. However, the computational power required to effectively run the algorithms clinically has not been available. For this reason alone, the comparatively computation-efficient FBP has been the preferred method.

The ordered subsets-expectation maximization (OSEM) method is an iterative reconstruction technique, which performs remarkably efficiently when compared to conventional iterative methods.[5] In OSEM, a subset of projections is used per iteration instead of the complete set. It uses an orderly selection of projections per iteration, so that maximum new information is provided.[6] Reconstruction times are proportional to the number of projections processed per iteration so if only four projections per subset are used instead of 128, OSEM will perform approximately 32 times faster. Surprisingly, although OSEM uses only a fraction of the available projection data per iteration, the rate of convergence between measured and observed data is approximately equivalent to that of the conventional iterative methods.

The majority of SPECT and PET vendors currently supply OSEM and its use is widespread. Its speed of reconstruction is slow compared with FBP (probably comparable to FBP five years ago), although it is an attractive alternative to FBP. As faster computers become available more complex modeling of attenuation, scatter, resolution, and noise should improve the accuracy of reconstruction.

INSTRUMENTATION

Gamma Camera Design

Introduction

As mentioned previously the fundamental detector system of the gamma camera has remained essentially unchanged through the 1990s. The gamma camera as a system has improved greatly as an imaging system. Much effort has been spent increasing study throughput. Quality control procedures have been streamlined. Processing is faster, but it is also more complex. Hospital-wide computer networking allows on-line, remote review and archiving of studies, and integration into hospital informatics means greater accessibility.

Gantry

The complexity of the gamma camera gantry is mainly because of its requirement to perform SPECT. Detectors with associated shielding and collimation weigh several hundred kilograms and they need to be moved closely and safely, around or along the patient. The orbit, especially in SPECT, must follow an exact path. Rotation of the heavy gantry with the requirement for precise angular movements results in complex acceleration and deceleration control using stepper motors. As well, patient safety necessitates a system that detects resistance to detector movement and touch sensitive surfaces. These requirements mean that much of the detector motion is under computer processor control.

Collimator resolution is depth dependent. Scan quality is improved if the distance between patient and collimator is kept to a minimum. Most current systems use patient-sensing technology, commonly photo-diodes, which either predetermine an orbit at set-up, or move detectors to a close position while scanning. This necessitates fail-safe mechanisms in respect to patient safety.

There have also been improvements in the manufacture of SPECT scanning beds or pallets. These pallets are commonly supported at one end (diving board style) and are relatively narrow to allow the detector to rotate laterally and posteriorly around the patient. They must be able to rigidly support

heavy patients while being relatively radiotranslucent. Fiberglass has been replaced by carbon fiber and Kevlar as the materials of choice.

Collimation

Background. Collimator design has remained relatively static over the last decade. The vast majority of collimators remain of the parallel-hole type.

The manufacturing of collimators has been refined and their quality in most instances fulfils the more stringent criteria for SPECT imaging. SPECT requires low variation in hole angulation. This was a concern in the early days of SPECT when collimators not specifically manufactured for the purpose were being used. Most collimators are currently produced using a casting technique that has improved robustness and uniformity when compared to foil-type collimators.[7,8]

As previously mentioned, collimator selection is a compromise between resolution and sensitivity. Most installed gamma cameras have at least two collimators to choose from, or more if the camera is to be used for imaging radionuclides with higher energy photons. Several physical parameters need to be considered when selecting a collimator. These are depicted in Figure 5.

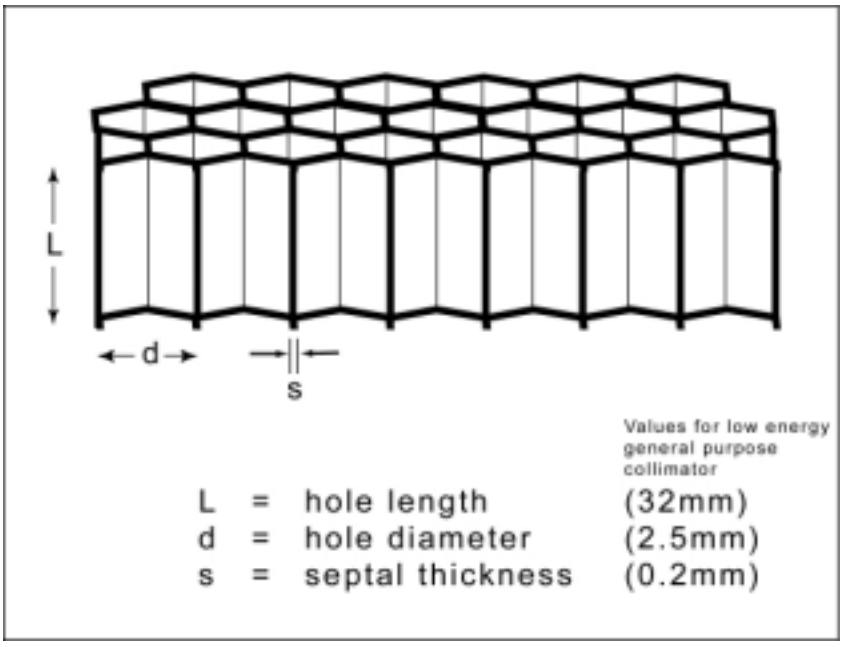

Figure 5. Cross-section through cast collimator with hexagonal holes.

Collimator sensitivity and resolution are defined as follows:

$$\text{Collimator sensitivity} = \frac{K_{\text{hole shape}} * d^4}{(L * (d + s))^2}$$

$$\text{Collimator resolution} = \frac{d * (L + H)}{L}$$

(Where H = source distance from collimator, and $K_{\text{hole shape}}$ is an equation constant determined by different shaped holes. For hexagonal holes, its value is 0.069, 0.080 for square holes, and 0.057 for circular holes).[38]

It is important to note from these two equations that sensitivity to activity (in the absence of attenuation) remains independent of scanning distance (H), whereas in parallel-hole collimators resolution is depth dependent.

Recent Innovations. While the above equations hold true for parallel-hole collimators, it is possible to enhance system resolution with the use of convergent

$$\text{Sensitivity} = (0.069 \times 2.5^4)/(32 \times (2.5+0.2))^2$$

$$= 0.00036$$

$$\sim \text{One photon per 2800}$$

$$\text{Resolution @5 cm depth} = (2.5 \times (32+50))/32$$

$$= 10.3 \text{ mm}$$

collimators. Convergent collimators are collimators where the holes point to a focus. The characteristics of these collimators are such that (i) as an object moves away from the detector it will appear to be magnified on the detector, (ii) sensitivity actually increases as the object moves away from the detector, and (iii) resolution at depth is enhanced when a suitable amount of convergence is employed. The distance to the point of convergence or focus is dependent on the application and the size of the detector but is typically 50cm. The main disadvantage of the convergent collimator is that the field of view gets smaller as the detector gets further from the patient. For this reason the applications for convergent collimators are limited, especially where truncation of the object by the FOV is intolerable (i.e., SPECT).

Typically, tomographic reconstruction is performed by reconstructing individual transaxial slices. These slices can then be 'stacked' to produce a volume of data. Reconstruction in tomography is complicated when the acquisition and subsequent back projection of data is not perpendicular to the axis of rotation (i.e., the back-projection path travels through multiple transaxial slices).

The fan-beam collimator (Figure 6A, 6D) has been developed for small FOV SPECT studies.[7,9] It combines improved sensitivity-resolution performance by being convergent in the transaxial plane while complying with reconstruction limitations by being parallel in the axial plane. SPECT reconstruction requires that the sides of the body being imaged are not truncated by the FOV, so the fan-beam collimator use is restricted to brain and pediatric work. The software used to reconstruct parallel-collimated studies does not need to be modified greatly to reconstruct fan-beam studies.

Cone-beam collimators (Figure 6B, 6D) are axially and transaxially convergent. In theory, they have excellent performance

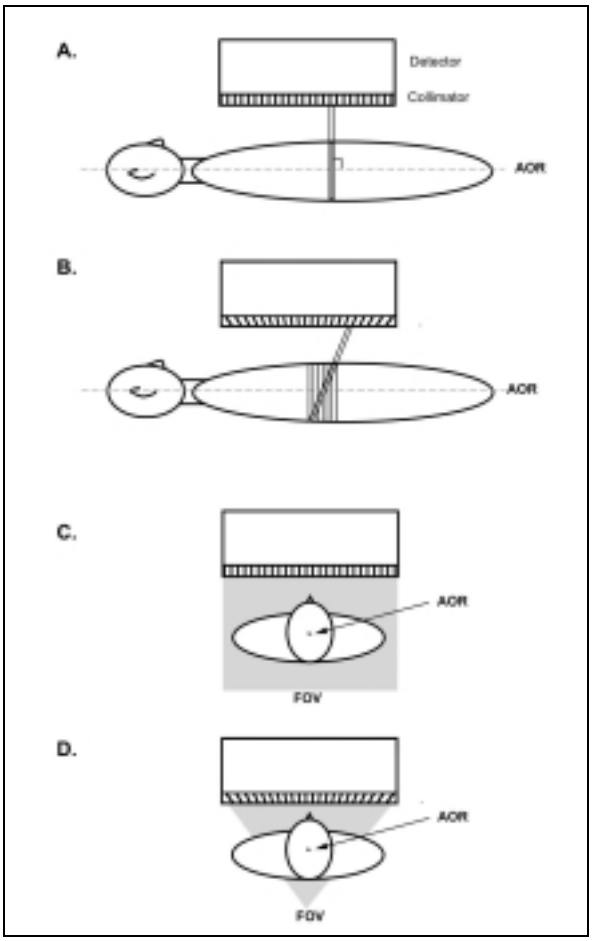

Figure 6. Design and FOV for parallel hole (A and C), fan-beam (A and D) and cone-beam (B and D) collimators in axial (A and B) and transaxial (C and D) planes. Convergent collimators have a reduced FOV that makes them suitable for small objects only (neurology and pediatrics); otherwise, FOV truncation of body may occur (see D). Cone-beam collimators that converge in the axial plane, result in more-complex tomographic reconstruction since the photon's path intersects multiple transaxial planes (B).

characteristics with very high sensitivity and resolution,[10,7] but they are difficult to implement and reconstruction is complex.

Multi-Headed Cameras

In a survey[11] of new gamma cameras installed in Australia in 1994-1996, 52% were dual headed, 16% triple headed, and

32% single headed. These figures will be similar to other markets. Multi-headed gamma cameras are a simple yet often expensive solution to system insensitivity. This approach reduces scanning time and/or improves scan quality.

Many multi-headed detectors are based on fixing multiple large field of view (LFOV) detectors on the one gantry. These systems are best suited to wide area surveys in both SPECT and planar imaging, but not all multi-headed gamma cameras have been designed in accordance with this philosophy. Systems optimized for specific types of imaging have also emerged. Myocardial SPECT requires a relatively small axial FOV. One manufacturer determined that the areas of the detector imaging superior and inferior to the heart (or other small organs) were being wasted and these parts of the detector could be better utilized as a second detector at the same axial level. This camera (GE Optima) effectively doubled the sensitivity of the single headed LFOV alternative, but didn't add greatly to the price.

Most early model dual-headed gamma cameras had fixed opposed detectors. These systems are ideal for 360° SPECT imaging and simultaneous anterior and posterior planar whole-body sweeps. However many centers perform 180°-SPECT when performing Thallium-201 myocardial studies. In this situation, imaging with fixed opposed gamma cameras has no benefits over a single headed gamma camera. Most dual-headed systems currently on the market are available in a variable angle configuration with detectors able to be set up 90° to each other for 180° SPECT. For this type of acquisition, the gantry rotates through 90° to achieve the most efficient utilization of both detectors.

Multi-headed gamma cameras require more complex geometric calibration as each detector needs to work in unison with the others.

Attenuation Correction

Background. The characteristic attenuation of photons by the patient's body makes it difficult to appreciate the distribution of radiotracer distribution. No other single factor restricts SPECT's ability to achieve absolute quantification of radiotracer distribution.

In many clinical studies, allowance for the pronounced effects of attenuation is required through knowledge of the patient's body habitus; without it the accuracy of the study suffers. One of the main purposes for attenuation correction is accurate reconstruction of myocardial perfusion studies. The heart position means that it is particularly prone to regional differences due to attenuation. It sits not only adjacent to lung tissue and mediastinum, but also at the base of the thoracic cavity where there is a large change in attenuation when moving inferiorly.

Corrections for attenuation in tomography are available and they are of two main types:

- Those that assume the attenuative nature of the body (first-order method), and
- Those that derive the attenuative nature of the body (transmission method).

First Order Attenuation Correction (Chang). Chang's method is used widely and is the most easily implemented.

The method calculates a restorative factor for individual pixels within a transaxial slice based on their relative position within the body.[7] Its failing is that it assumes a homogeneous attenuation environment within the body. This is a significant issue, especially in areas such as the chest, in which there is bone, soft tissue, air, and lung. Thus, it is useful only when there is relative homogeneity in attenuation (e.g., abdomen, pelvis and brain). In areas of the body in which counts are different due to regional differences in attenuation (e.g., in myocardial perfusion studies), the relative

differences will be maintained following correction.

The first step is to determine the boundary of the body. The depths of individual pixels within transaxial slices are calculated at each projection angle. The attenuation correction factor applied to a pixel is the inverse of the average of the attenuation factors obtained at each projection angle.

Measured Transmission Attenuation Correction. Some of the early research into SPECT attenuation correction was performed using co-registered CT and SPECT studies. Attenuation coefficients were extrapolated from the CT Hounsfield values.[12,13] There were many problems, including the accurate alignment of CT and SPECT studies, and the errors in the approximating of linear attenuation coefficients from CT values. Interestingly, current work in progress from one manufacturer is hoping to use a combined SPECT and CT system for this application.

An accurate attenuation map of body tissue can be determined by performing a transmission study akin to CT but using a radioactive source. Early techniques used a flat flood source of radioactivity mounted to the detector and on the opposite side of the patient (Figure 7A).[14] It showed the potential for measured transmission attenuation correction (MTAC) but it added greatly to the time of the study.

Some of the factors that need to be addressed in providing accurate and effective MTAC are:

- **Source selection** – ideally a source with similar photon energy to the emission radionuclide is used. This allows for the most accurate attenuation coefficient calculation, and means that the detector performance is matched between emission and transmission studies.
- **Signal separation** – The acquisition of both signals (emission and transmission) must be separable and cross-contamination minimized. Signal separation can be achieved by doing the transmission study on the patient before radionuclide administration. However, this isn't practical in many types of studies where there is a prolonged uptake phase (e.g., bone scanning) or where other factors determine the administration of the radionuclide (e.g., myocardial stress studies). A common method of signal separation is to use a transmission source with a photon whose energy is similar to the emission photon but separable by energy discrimination. Simultaneous acquisitions of transmission and emission signals can be performed but down-scatter from the upper to lower energy window needs to be allowed for. Another method is to dedicate one detector of a multi-detector camera to acquiring the transmission data.
- **Exposure to source** – Ideally the source should be shielded when not in use. Exposure to patient and operator should be kept to a minimum. The half-life should be suitably long so as not to require frequent handling or costly replacement.

Moving Line Source. One common approach is to use the "moving line source" technique for MTAC (Figure 7B). From a practical point of view, it would be optimal to perform emission and transmission studies simultaneously, but as mentioned above the signals must be separable and not compromised by downscatter.

With this technique, a line source collimated to only project photons through the patient perpendicular to the detector collimator sweeps across the FOV at each SPECT projection frame. A position de-coder attached to the line source tells the detector where at a particular time the line source is and extracts from the gamma camera's signal the line of image data (around 50 mm wide) that reflects the transmission signal. Other areas of the

gamma camera's image that don't contain transmission source counts are stored as emission data.

The advantage of this system is that the transmission signal can be confined to a target area leaving other areas of the FOV unaffected for collection of emission data. The strength of the transmission signal can be increased so that the contribution to it by emission signal is trivial.

A further improvement may be gained by combining fan beam and moving source technologies, by moving a point source along the focal line of a fan-beam collimator (Figure 7D).[15]

Multi-Detector Systems. In multi-detector gamma cameras, one of the detectors may be dedicated to acquiring transmission data. Moving line source techniques are difficult to implement when there are opposing detectors. A solution is a fan-beam collimator with a line source positioned at its foci (Figure 7C).

This is easily implemented on triple headed gamma cameras, and has even been developed on gamma cameras with opposing detectors using an asymmetric fan-beam system.

Dedicated PET Camera Design

Introduction

PET involves the detection of the 511 keV annihilation photons that are emitted in near opposite directions following positron decay. Interestingly, as PET devices improve in resolution some of the characteristics of positron decay are more often seen as the resolving limit of this modality.[16]

PET imaging assumes that if two annihilation photons are recorded in coincidence on opposite sides of the patient then the nucleus from which the positron undergoing annihilation originated must be on a straight line between the two points of detection. This line is known as the line of response (LOR). Two properties impact on this assumption. Firstly, the positron has energy, which it loses during collision with the orbital electrons of surrounding tissue. Once it has lost most of its energy, it annihilates with an electron to form a positronium. Its range depends on the energy of its emission (ß$^{+}$ E_{max}), which is nuclide dependent. The estimated effect on PET imaging resolution is approximately 0.2 mm FWHM for 18-F (ß+ E_{max} = 0.64Mev) and 4.5 mm for Rb-82 (ß+ E_{max} = 3.35MeV).

Secondly, annihilation photons aren't emitted in exactly opposite directions. Photon non-colinearity amounts to

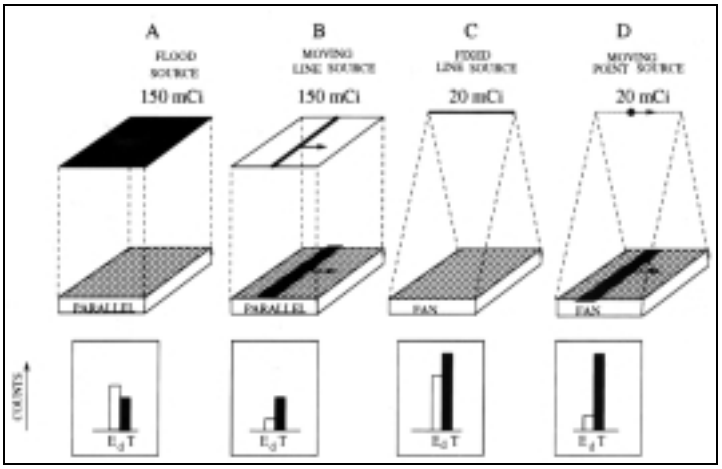

Figure 7. Comparison of the geometry of various transmission configurations (top row) for attenuation correction in SPECT.[15] The bottom row shows the relative sensitivity (T) for the source activity stated. Downscatter from the emission isotope (99m-Tc, 140 keV) into the transmission window (153Gd, 100 keV) was calculated (E_d), and related to the transmission counts for each geometry. Best results are achieved when transmission sensitivity (T) is highest and relative emission downscatter (E_d) is lowest. High transmission sensitivity has the added benefit of reduced source activity and therefore inexpensiveer purchase and replacement costs. (Reprinted with permission of the Society of Nuclear Medicine from: Beekman FJ, et al. Half-fanbeam collimators combined with scanning point sources for simultaneous emission-transmission imaging. *J Nucl Med.*1998; 39:1996-2003.

approximately 180° ± 0.25°. The effect of non-colinearity on PET imaging resolution depends on the separation of the detectors. In a typical camera, the resolution loss is about 2.1 mm. The small-diameter detector ring of small animal PET scanners means that this effect is reduced.[17]

Detector Selection, Design and Properties

Historically PET cameras have used BGO crystals as small discrete detectors in a ring. The size of each crystal element is the major determinant of system resolution. For a 6 mm square detector element the geometric resolution is 3 mm in the center of the FOV.[18]

The best intrinsic resolution in PET detector ring is achieved at the center of the FOV. The rate of deterioration in resolution away from the center depends on the diameter of the detector ring. Photons emitted further away from the center of the FOV are more likely to hit the crystal elements at an angle (Figure 8), which produces a greater positional uncertainty due to a parallax error. Note that as the ring diameter increases there is less degradation in resolution as you move further away from the center, although the non-colinearity error increases.

Research is being undertaken to determine where, along the length of a crystal, a photon is absorbed. This is known as "depth of interaction."[19,16] Estimates suggest that if the depth of interaction could be calculated accurately to one-third of the depth of the crystal; parallax error, as described in Figure 8, could almost be eliminated.[18] Depth of interaction calculations can be performed with the use of

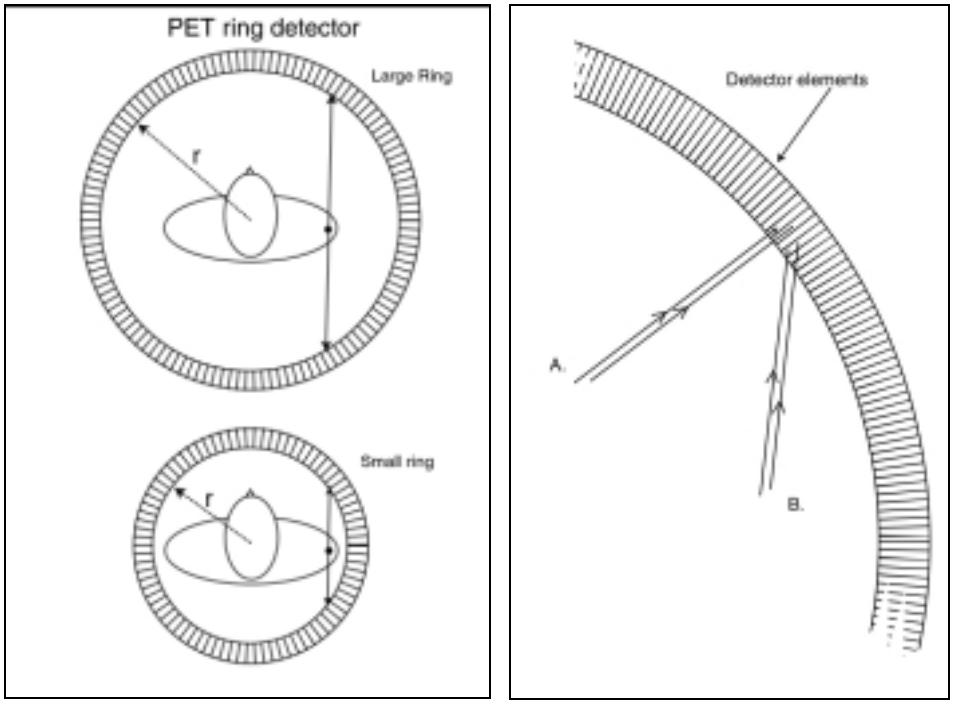

(i) (ii)

Figure 8. PET ring detector. (i) Detector elements, which are typically 30 mm deep and 6 mm square, are mounted radially around the detector. Photons traveling from the center of the FOV will hit the element parallel with its longest dimension. As the distance increases from the center of the FOV, a parallax error occurs which affects resolution. The parallax error is greater in scanners with smaller radii and hence degradation of resolution is greater. (ii) Loss of resolution away from the center of the FOV is caused by parallax error. Two photons from separate sources (A) can be resolved because they are detected in adjacent elements. Two photons from separate sources cannot be resolved if they are detected in the same element (B). The parallax error increases as the distance increases from the center of the FOV. Determining the depth of interaction within in the crystal element can reduce the error.

light measuring photo-diodes at the patient end of the crystal, which determine in which of the elements within a detector module an event has occurred. This is then compared to the amount of light seen by a single PMT at the opposite end and from their ratio, the depth of interaction within the crystal is calculated. Detector modules like the one shown in Figure 9 are being developed to allow depth of interaction calculation.

The ability to calculate depth of interaction will enable the diameter of the detector ring to be reduced, decreasing the number of detectors (and cost). It will also reduce the deterioration in resolution caused by annihilation photon non-colinearity.

The recent development of Lutetium Oxyorthosilicate (LSO) crystals may impact on detector selection. LSO has many properties that make it more suitable for PET than BGO. Of particular importance are more efficient light photon production and a shorter light decay constant. This should result in better energy resolution that will reduce the contribution of scatter. As well, increases in the amount of light produced per scintillation should mean that each detector module could be cut into smaller elements, as the signal will be sufficiently strong to allow more accurate determination of its position of interaction.

There is also potential, due to the high light output, for an LSO detector to be manufactured in larger detectors using similar logic to the gamma camera. Such a detector would need to be able to handle very high count-rates and this should be possible with the short light decay constant of LSO.

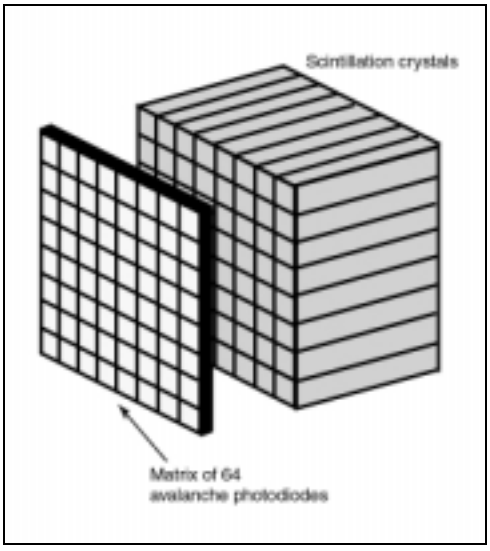

Figure 9. PET detector module with matrix of photodiodes for calculating 'depth of interaction'. The module uses a single conventional PMT (not shown) at the opposite and rear ends of crystal elements. The crystal element where scintillation occurs is identified by a single photodiode within the matrix. Ratio of signals between photodiode and PMT reflects "depth of interaction."

2D vs. 3D Acquisition

For many years, PET scanners acquired images in 2D mode using ring shaped septa to restrict coincidences to one of many transverse planes. In doing so, these coincidences were acquired and reconstructed in the one transverse section. Researchers recognized the inefficiency of this mode of acquisition and attempted to increase sensitivity by removing the septa (Figure 10).

When septa were removed, there was a dramatic increase in sensitivity (500%), unfortunately accompanied by a dramatic increase in the scatter fraction (from 10% to 35%). In 2D acquisitions scatter contribution is mainly confined to photons that remain in the same transaxial plane following collision, as otherwise they will be absorbed by the septa. In 3D acquisitions, photons scattered in any direction have an unimpeded path to the detector.

The increased sensitivity of 3D acquisitions is attractive for a number of reasons.[37] A large proportion of patients are volunteers in whom the radiation dose is quite consequential. Ethical approval often demands restrictions in the number of scans performed and the dose administered to these

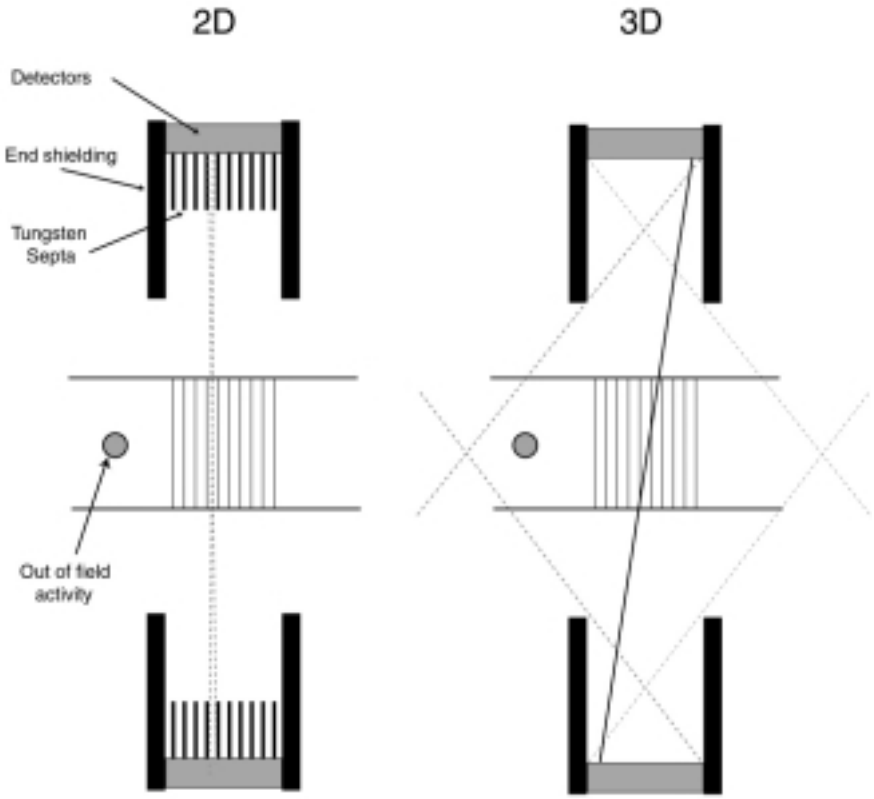

Figure 10. Axial cross-section through PET scanners in 2D and 3D modes.

groups. Many studies are also undertaken using tracers with low uptake and on whom dynamic studies result in short acquisition intervals. 3D acquisitions are often employed in such studies to improve image quality by reducing statistical noise.

Problems arising from 3D PET acquisitions include:

- The increased scatter fraction requires more extensive and vigilant correction.
- The detectors are no longer shielded from "out of field" activity. Hot structures such as the brain and bladder can contribute significantly to random and scatter fractions.
- In 2D PET, there is consistent sensitivity to activity along the axial plane. In 3D PET, the axial acceptance angle for coincidence decreases closer to the ends of the FOV. Axial normalization is required to correct for this reduced response, however, reduced sampling means that there is greater noise. When acquiring multiple bed position whole-body studies, 3D PET systems typically overlap by half the axial FOV to achieve constant sam-pling and noise along the axial plane.
- Coincidences detected are no longer confined to a single transaxial plane. The LOR of a coincidence can intersect many transaxial planes. This requires either approximation of the data to a transaxial slice (single slice rebinning) or complex 3D reconstruction algorithms not dissimilar to those required for conebeam collimated SPECT.

In 3D scanners, scatter contribution is primarily eliminated through energy discrimination. The commonly used BGO scintillator has relatively poor energy resolution and therefore a future replacement scintillator should have better energy resolution to be able to take advantage of 3D technology.

Attenuation and Scatter Correction

Background. Despite the penetrating nature of 511 keV photons when compared to the low energy photons used in the majority of conventional nuclear medicine studies, PET scanning is subject to pronounced attenuation by the patient. PET requires the detection of two single 511 keV photons in coincidence; the attenuation effect on those two single photons is therefore compounded. The half layer value for 511 keV

photons in water is approximately 7 cm. This means that 511 keV photons emitted from a point in the middle of a water-filled cylinder with radius of 7 cm have a 50% probability of exiting the body without being attenuated. However, the overall probability of detecting both photons in coincidence is only 25%. In a cylinder with 14 cm radius (which is not dissimilar to the average human torso) the probability of remaining unattenuated is 6.25% (0.25 squared). The equivalent value for 140 keV photons in SPECT would be 12%. Figure 11 shows that the effect of attenuation on 511 keV coincidence imaging is more pronounced than that on 201-Tl SPECT imaging.

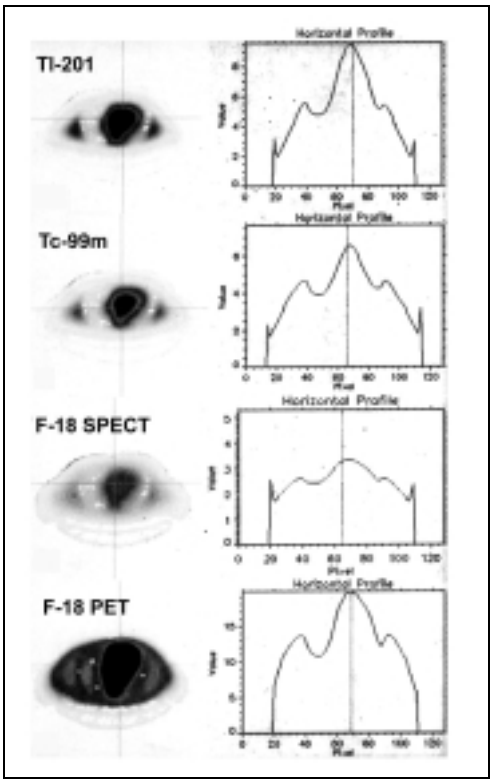

Figure 11. Left column shows the attenuation correction images for attenuation applied to different radioisotopes imaged with SPECT and PET of a phantom. Right column shows count profiles graphs. Actual restorative values for correction of attenuation are displayed in the y-axis. Central maximum restorative factors for Tl201, Tc99m, F18-SPECT, and F18-PET are 10,6,3 and 20 respectively. (Figure provided courtesy Dale Bailey, Hammersmith Hospital, UK.)

The established method for performing transmission correction in PET cameras uses positron emitting rod sources of relatively long half-life isotopes for transmission sources. These are rotated 360° around the patient and the density of recorded coincidences reflects attenuation in the patient. The algorithm that reconstructs transmission data uses the same principles as CT reconstruction and the resultant images are comprised of attenuation coefficients. Germaniun-68 (T1/2 =270 days) sources are typically used and are retractable when performing an emission study.

Post-Injection Transmission Studies. As emission and transmission signals hitting the detectors are both 511 keV photons, early PET scanners needed to perform the transmission study prior to dose administration to the patient and the patient needed to remain stationary during transmission, uptake and emission periods. For studies with long uptake times, this was quite difficult and resulted in inefficient use of camera resources.

The ability to perform post-injection transmission studies became available with the development of a technique that was capable of predicting geometrically whether a coincidence originated from the patient or transmission source. It achieved this by recording whether a LOR intersects with the position of the transmission source as it rotates at the moment of detection.[22] If a photon doesn't meet these criteria it is rejected (Figure 12i). Some emission coincidences may accidentally intersect with the source but their contaminating contribution is negligible (<1%). This technique has been refined to the point where transmission and emission studies can be performed simultaneously.

Singles Transmission. A limitation of PET systems that operate close to their maximum count-rate capability is dead time loss due to the rod source passing close to the detectors during transmission scanning. This can lead to significant image degradation if the source is too radioactive.

An alternative is to use a 'singles' source, usually Cesium-137 ($T_{1/2}$ = 30 years, gamma=660 keV), which is collimated to project a fan beam of radiation through the patient towards the detectors opposite, and is retracted when not in use. Shielding protects detectors adjacent to the source and hence a much greater activity can be used when compared to positron sources (Figure 12ii[a]). A pseudo-coincidence is formed between the source and the detected event.[23] The transmission signal can be differentiated from the emission signal by energy discrimination (Figure 12ii[b]) so that post-injection transmission scanning can be performed.

An additional benefit is that due to the long half-life of Cesium-137 there is no recurrent expense of source replacement.

Transmission Image Segmentation. One issue with transmission attenuation correction is that it is achieved through an arithmetic operation between two sets of images that contain noise,[1] which leads to a corrected image whose noise component is higher than that of either of the emission or transmission images. Transmission images contain pixel attenuation coefficient data. Segmentation is a technique that reduces noise dramatically in areas of uniform attenuation, by giving all pixels the same attenuation coefficient. Typically, all soft tissue equivalent values are segmented, while others such as bone and lung use the measured value.

Scatter Correction. In 3D PET of the chest, it has been estimated that 50% or more of detected coincidences have undergone some Compton scatter within the body.[24] This compares to a scatter fraction of 10-15% in 2D PET with septa.

As with SPECT one of the major factors contributing to acquiring scattered photons is detector energy resolution. Poor energy resolution leads to increased scatter contribution. Shielding can also reduce scatter. The septa rings used in 2D PET acquisition drastically reduce scatter, but they also reduce system sensitivity by a factor of five.

Correction for scatter contribution is usually performed by measuring the counts

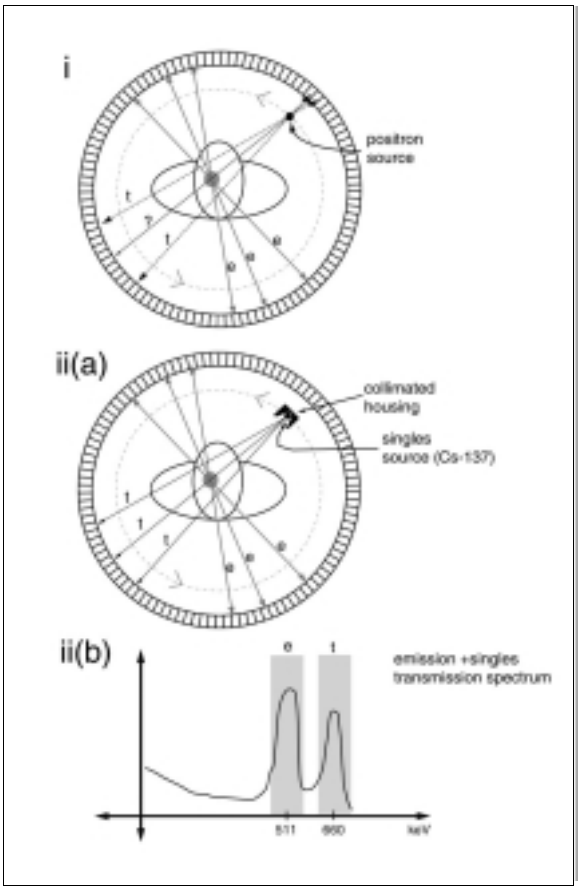

Figure 12. Transmission attenuation correction in PET.

(i) Post-injection technique with rotating positron rod source. LOR is deemed to be from the transmission source ('t') if it intersects with it. A small percentage (<1%) of emission ('e') LORs will be incorrectly recorded as transmission LORs.

(ii) (a) Singles attenuation correction with rotating collimated Cesium-137 point source. (b) Separation of transmission and emission photons by energy discrimination.

outside the body. Techniques can determine the amount of counts contributed by scatter within the patient by measuring and extrapolating counts from outside the patient.

New techniques are being developed which model the scatter component in the emission image based on the transmission images and subtract its contribution.

Partial Ring BGO PET Scanners

The development of 3D acquisition techniques for PET scanning meant that counts achieved were sufficiently great to contemplate reducing the number of detectors. The primary motivation was to manufacture a PET scanner at greatly reduced cost (Table 4) (Siemens ECAT ART, CTI PET Systems, TN).

A scanner[20] was developed which comprised two banks of opposed detectors, each spanning 82.5°. No septa were installed so acquisitions were restricted to 3D.The detectors were BGO modules and identical to those used in a full ring PET system capable of 2D and 3D acquisitions (Siemens ECAT EXACT, CTI PET Systems, TN, USA). The detectors are fixed on a slip ring that rotates

Table 4. Comparison of Commercially available PET systems. Each example is approximately representative of market competitors [1,20]

	Dedicated Full ring BGO*	Dedicated Partial ring BGO†	Dedicated Full ring NaI(Tl) ‡	Coincidence Gamma Camera§
Crystal dimensions Width x length X depth (mm)	3.9x8.3x30	6.5x6.5x20	500x300x25	510x380x15.9
No. of crystals (or elements)	12K	4.2K	6	2
Detector diameter (mm)	93	82	90	66
Transaxial Resolution (mm)	4.8	6.3	5.8	4.8
Scatter fraction (%) 3D(2D)	35(10)	32	27.8	26
Sensitivity (cps/Bq/ml) 3D(2D)	27.0 (5.4)	7.5	12.4	3.7
Crystal volume (cc)	11800	3570	22000	3081
Axial FOV (cm)	15	16.2	25	34
Approx. cost US $	2,000,000	1,300,000	1,200,000	120,000 (Coincidence detection option) 400,000 (Gamma camera)

*GE Advance (GE Medical Systems Inc)
†Siemens Exact ART (CTI/Siemens)
‡ ADAC C-PET (ADAC Laboratories)
§ADAC MCD (ADAC Laboratories)

at 30 rpm, and during acquisition, the ring rotates continuously.

Comparing the systems found that the 3D partial ring system had approximately one third the sensitivity of the full-ring system in 3D mode, but twice the sensitivity of the full-ring system in 2D mode.

Further cost savings are made in this model by using BGO crystals with a depth of 20 mm (cf. 30 mm in most high-end PET systems).

Dedicated NaI(Tl) PET Scanners

Despite its relatively poor 511 keV photon stopping power, one group persists using NaI(Tl) for dedicated PET scanners (UGM/PennPET) with very good results.[25] The advantage of NaI(Tl) is that it has very good light output per interaction, and it is inexpensive.

One of the unique features of this system is that it uses large crystal detectors of gamma camera proportions, in contrast to BGO PET scanners where small crystal elements are the smallest resolving unit. Resolution is not therefore restricted to the physical dimension of these elements.

The PennPET scanner consists of six such detectors with PMTs arranged around the patient, with an axial FOV of up to 250 mm. The geometry is akin to a 6-headed stationary gamma camera with crystals fixed as close as possible to each other. Crystal thickness is 25 mm, which is approximately twice as thick as those used by conventional gamma cameras. This gives it an efficiency of 56% for 511 keV photons and 32% in coincidence, which is well short of BGO performance in comparison at 90% and 81%, respectively.

In has achieved good performance and a niche in the market by addressing some of the problems associated with NaI(Tl) in coincidence mode.

A major hurdle and remaining limitation is the maximum countrate achievable. The detector operates exclusively in 3D mode without shielding between patient and detector. In SPECT the detector is protected from the vast majority of radiation emerging from patient by the collimator and dead time loss is rarely an issue. Typically, clinical count rates rarely exceed 10 Kcps and dead time loss becomes an issue when count rates exceed 50 Kcps. The PennPET scanner typically operates at 500 Kcps per detector or 3 Mcps for the whole system. These rates are typically observed in the 250 mm axial FOV scanner an hour following 3 mCi (111MBq) of FDG. High count rates are achieved through two innovations, which are a departure from Anger logic that has serviced conventional gamma cameras for 30 years:

1. When scintillation occurs in a gamma camera the light produced is detected and measured by all PMTs of the detector. During this time (dead time), the system is effectively paralyzed from detecting further events. The PennPET scanner circumvents detector wide dead time by dividing each detector in 3 overlapping “virtual” detectors that can operate independently (Fig.13A). Determination of the position of an event is restricted to the closest PMT and surrounding six PMTs.
2. Clipping the electrical signal from the PMT after 150nsec further reduces dead time. Sufficient light is produced by the NaI(Tl) crystal to forego the signal in the latter section of the pulse (Figure 13B). Accurate energy calculation is obtained by integrating the area under the early section of the pulse.

These two innovations increase by an order of magnitude the maximum operating count rate of these detectors compared to Anger type systems. The technology of the UGM/PennPET system was subsequently applied to dual headed gamma cameras, and the manufacture of the first commercial

hybrid PET/SPECT gamma camera (ADAC Laboratories, MCD).

Count rate limitations make this scanner unsuitable for short half-life studies that typically scan following bolus administration of greater than 30mCi, but are well suited to relatively steady state studies like those with FDG.

This group has further improved system performance with the use of six curved detectors, which are formed into a circular arrangement.[26,27]

Time-of-Flight PET Detectors

When 511 keV photons are detected on opposite sides of an object within a defined time window, they are deemed to form a coincidence. This coincidence is recorded as a LOR and the nucleus from which the event originated is predicted to have arisen from somewhere along this line.

Normally the coincidence window is 5 ns to 15 ns. This window is long enough to allow for sampling errors in the timing of events, but short enough to exclude random coincidences. The detector property that impacts most on the accuracy of timing of an event is the photon decay constant.

If the timing of detected events can be determined with sufficient accuracy then the position along the LOR from where the annihilation photons originated can be calculated by looking at the different arrival times at the detectors. In a perfect time-of-flight system a coincidence of events would ultimately be recorded as a count in a voxel and obviate the need for tomographic reconstruction. Current technology allows for a minimum timing resolution of around 0.3ns, which equates to around 5cm along the LOR. This amount of timing resolution would still require acquired data to undergo tomographic reconstruction albeit in a constrained manner.[39]

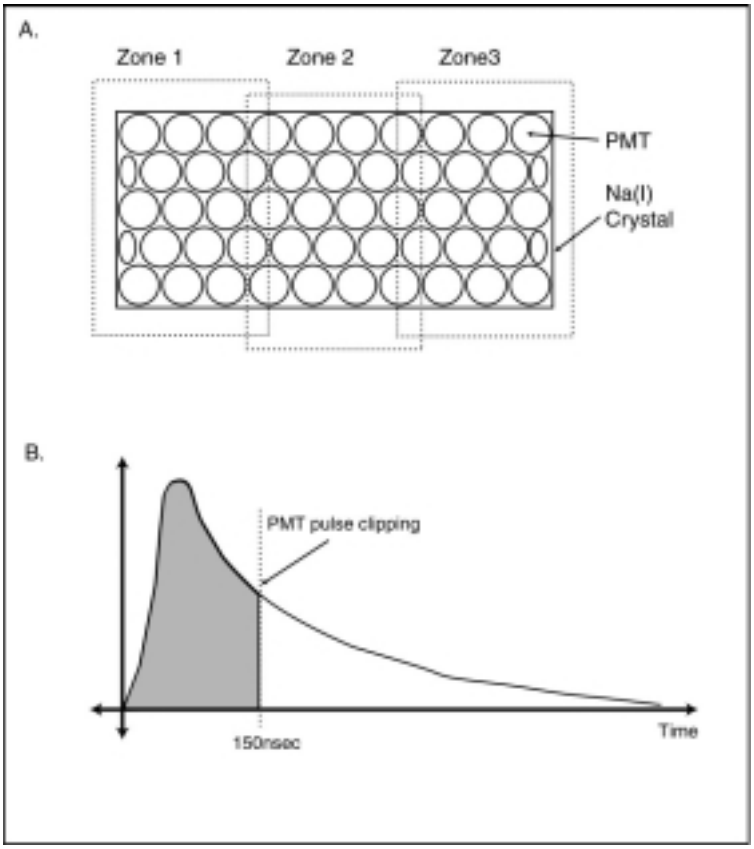

Figure 13. NaI(Tl) detector modifications. Single detector zoned into separate “virtual” detectors that operate independently. Photon scintillation processed by closest PMT and six surrounding PMTs only. Dead time effectively restricted to zone and not whole crystal. A. PMT signal is clipped after 150 nsec and energy integrated under early section of pulse, thus reducing dead time.

Barium Fluoride (BaF2) has appropriately short photon decay constant (0.8 ns), but it suffers from relatively poor light output, a wavelength not suited to conventional PMTs and poor photon stopping power.

Time-of-flight detection may be possible with LSO. It has a photon decay constant of 40 nanosec, which is much longer than BaF2, however, event timing of sufficient accuracy may be possible to allow time-of-flight detection.[40]

Multi-Modality Cameras – Marriage of CT and PET

Much of the research into the clinical efficacy of PET has identified that improved accuracy of diagnosis is markedly improved by combined observation of PET (functional imaging) and CT (structural imaging), as opposed to each modality in isolation. To improve the combining of modalities, digital co-registration of functional and structural images is pursued by many clinicians; however, this is difficult to achieve with any accuracy due to the studies being acquired during different sessions under different conditions and unavailability of images in a digital format.

A system that combines high performance PET and spiral CT in the one scanner system should be on the market soon.[28] It is essentially a PET and CT scanner bolted together with a common scanning bed. It will provide the facility for accurate co-registration and potentially allow CT to supply PET with transmission images for correction of scatter and attenuation. It will also allow PET data to be combined with CT for radiotherapy planning and include function as a basis for treatment rather than structure alone.

Such systems do not acquire their data of the same tissue simultaneously. Scans are usually acquired end-to-end albeit in the same session. There is still potential for mis-registration of function and structure due to patient movement or changes in the anatomy of the patient (eg. filling bladder or moving small bowel).

In the future a scanner may be developed which is designed as a combined scanner which can simultaneously acquire functional and structural data rather than as separate units bolted togeter.

Future Developments in PET Scanners

Much of the future of PET scanning will rely on the selection of a replacement for BGO. BGO is the current crystal of choice in high-end dedicated PET scanners; however, over the last few years LSO has emerged as a replacement with more desirable physical properties. Its greater and faster photon production properties, compared to BGO, should allow the construction of smaller crystal elements and therefore better system resolution, and allow accurate 'depth of interaction' calculation. Despite this, its energy resolution in a standard configuration isn't any better than BGO. As mentioned previously energy resolution is an important property in the control of scatter contribution, especially in 3D scanners.

The GSO scintillator offers good energy resolution and may be less expensive than the LSO. A dedicated PET camera using this detector material is about to released on the market.

Tomographic reconstruction of 3D acquisitions is being improved with several techniques now available that perform true 3D reconstructions, as opposed to approximation (or rebinning) of data into 2D.

The physical joining of PET scanners to CT (or even MRI) should improve the accuracy of diagnosis in many clinical areas, and assist in surgical and radiotherapy planning. Although not completely realised yet, the potential for accurate attenuation and scatter modeling from acquired CT data shows promise.

Hybrid SPECT/PET Gamma Camera Systems

Introduction

Currently most manufacturers are offering coincidence based gamma camera systems capable of performing PET. Although performance specifications are inferior to dedicated PET scanners and the future holds promise for what is a young technology.

The ability to perform both SPECT and PET on the one scanner is economically

attractive. PET scanners usually experience considerable down time due to unavailability of dose, especially in departments without on-site cyclotron facilities. Hybrid cameras are available for SPECT imaging at these times.

Capital investment is appreciably less than for dedicated PET (Table 4). The coincidence detection option for most of these types of cameras is approximately US$120K on top of the gamma camera cost of US$400K. This compares favorably with the cost of high end dedicated PET of approximately US$2000K.

There has been considerable debate on the merits of hybrid and dedicated PET scanners and a great deal of analysis of their respective physical performance.[29] Scan quality of hybrid scanners is less than that of dedicated PET scanners. This impacts most in the detection of small volume disease or where there is low contrast, especially in areas of the body subjected to more attenuation (e.g. abdomen). Unfortunately, access to PET imaging is limited in many health regions. Often the debate isn't whether a study should be performed on a hybrid or dedicated PET camera, but whether any PET scan is available to the patient. In this situation and with knowledge of their limitation, hybrid scanners may play a role in some applications.[30]

Some consensus has been reached following clinical testing. Hybrid cameras show best performance in areas of the body that aren't subjected to great amounts of attenuation. It shows best results in head, neck, and thorax. In a comparison of hybrid and dedicated PET in detecting suspected body malignancies,[31] gamma-camera-based PET found 78% of all lesions seen on dedicated PET. This value equates to 83% in the thorax but only 67% for subphrenic lesions. In the 10 lesions missed by hybrid PET 8 were <1.5 cm and 2 cm were deep in the abdomen. Interestingly the resolution specifications of the two scanners showed the hybrid scanner had 5 mm and dedicated scanner 6.5 mm, while sensitivity was a factor of 12:1 in favor of dedicated PET.

These results are reflected in a paper by Shreve et al where coincidence gamma camera PET detected 55% (66/105) of lesions detected by dedicated PET in a wide range of malignancy types and locations.[32] Of mediastinal lesions >1.5 cm in diameter it detected 94% (15/16), but only detected 30% of these lesions where the diameter was less than 1.5cm. The hybrid camera performed well in other areas apart from the abdomen where it only detected 23% (6/26) of lesions.

Hybrid scanners usually operate in an open 3D mode and are subject to the effects of out of field activity. Resolution measurements are similar to dedicated PET scanners but hybrid scanners suffer from lower sensitivity and higher scatter fractions. Low detector sensitivity is exacerbated by incomplete or partial geometry.

Design Considerations

One of the main restrictions to the use of gamma cameras for PET has been handling the very high count-rate experienced following the removal of collimators. Typically, the detector count-rate for PET is 50 times higher than that for routine SPECT.

Higher count-rate capability is achieved by the techniques described in previously. These include pulse clipping of the PMT signal, and calculation of the position of detected events that are restricted to local PMTs. These two innovations allow detector count rates of greater than 500Kcps to be achieved and were originally adapted from the PennPET NaI(Tl) scanner into the first commercially available coincidence gamma camera.[33] Other manufacturers have introduced various innovations to process the high count-rates arising from detectors and PMTs.

There are also issues related to the ability of a crystal whose thickness is optimized for lower energy photons to detect 511 keV photons in coincidence with any efficiency. Increasing crystal thickness improves efficiency in PET mode but degrades the intrinsic resolution (and therefore system resolution) in SPECT mode. As PET relies on the detection of events in coincidence improving the efficiency of a single detector has a square effect on coincidence efficiency. Doubling efficiency in singles photon mode has a quadrupling in coincidence efficiency.

As stated in previously, system resolution is defined by intrinsic resolution and collimator resolution. Degradation in intrinsic resolution due to increasing crystal thickness has a small effect on system resolution, but many argue as to what is tolerable.

Future Developments in Hybrid Scanners

LSO. There has been a degree of excitement amongst the nuclear medicine community with the possible use of LSO in hybrid gamma cameras. Its superior stopping power and fast light photon properties would make it an excellent replacement for NaI(Tl) when operating in PET mode acquisitions. It has superior sensitivity to NaI(Tl) at half the crystal thickness.

A problem with LSO is that it is inherently radioactive (containing naturally occurring Lu-176), with emissions in the SPECT photon range.[34] To counter this problem a thin layer of a second type of crystal suited to SPECT (YSO or NaI(Tl)) could be optically coupled to the front of an LSO crystal. This veneer of crystal is designed to detect lower energy SPECT photons, while the majority of 511 keV photons will penetrate this layer to be detected by the LSO layer. In SPECT mode, scintillations in the front crystal can be characterized and differentiated from the scintillations occurring because of photons emitted from within LSO due to radioactivity. When operating in PET mode the front layer would be penetrated by the vast majority of 511 keV photons, leaving them to be absorbed by the LSO layer.

A factor in the success of hybrid gamma cameras is economics. LSO is by comparison much more expensive than NaI(Tl) (see Table 3(m)) and this will impact greatly on the overall cost of the scanner. In SPECT mode, especially for photons with energy <200 keV, there is unlikely to be sufficient improvement in image quality to justify the increased cost over NaI(Tl).

Slotted Integral Crystals. Poor sensitivity due to poor detector efficiency is one of the major limitations of hybrid systems in PET mode. Increased crystal thickness improves the efficiency of detecting 511 keV photons, but thicker crystals degrade intrinsic resolution in SPECT mode. Resolution degradation results from greater spread of light photons following scintillation. Spreading of light over a greater area decreases the accuracy with which the origins of that light, photon absorption and scintillation, can be calculated. Crystals for SPECT systems are generally 3/8" to 1/2" thick.

As stated in previously, doubling the efficiency of detecting single events results in a four-fold improvement in detecting coincidences.

A way of improving the resolution characteristics of thicker crystals is to crisscross the PMT surface with thin slots of a depth approximately half the total crystal thickness (Fig.14). The slots, which are approximately 1/2" apart, are designed to reduce the radial spread of light following scintillation, and channel the lights towards the PMTs.

An additional benefit is an improvement in image quality when scanning high-energy photons in single photon mode (e.g., I-131).

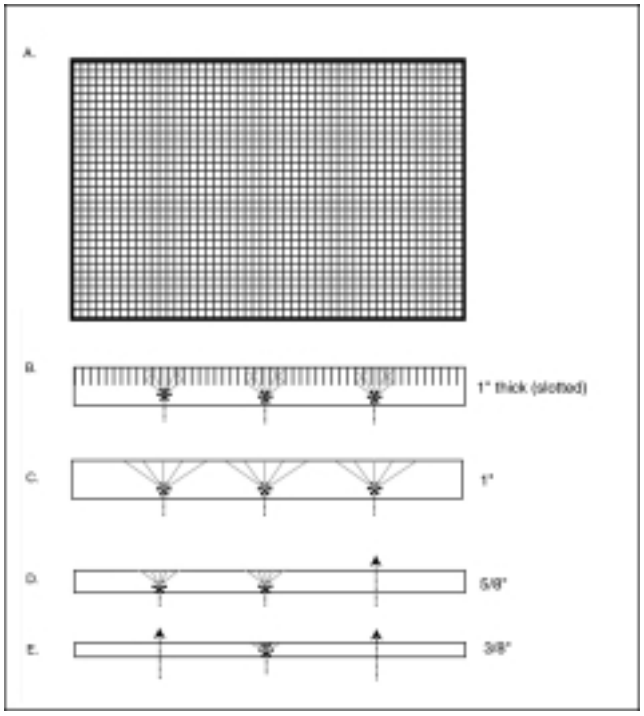

Figure 14. Slotted NaI(Tl) crystal showing reduced light spread compared to unslotted crystal of equivalent thickness, and hence improved intrinsic resolution.

A. Top view of crystal
B. Slotted 1" crystal
C. Plain 1" crystal with greater light spread, and equivalent sensitivity.
D. Medium crystal (5/8") with less light spread but less sensitivity to high-energy photons.
E. Thin crystal (3/8") with even less light spread and therefore excellent resolution, but poor sensitivity to medium and high-energy photons.

CONCLUSIONS AND THE FUTURE

Many readers of this manuscript will have noticed the current dominance of PET in this topic. Despite its age, PET is undergoing radical change in almost every aspect of the modality, from the basic detector through to clinical applications. Future developments in instrumentation will focus on new scintillation materials, the implementation of depth of interaction analysis, and improved energy resolution for 3D mode of acquisition. This should allow cameras of exceptional resolution (2mm) to emerge at the high end of the market, potentially married to CT or even MRI scanners. Other markets will ensure that hybrid PET/SPECT camera technology continues to develop.

New detector materials and designs being investigate for hybrid PET/SPECT cameras may produce spin-offs that are manufactured into, and improve conventional gamma cameras. Due to collimation, it is unlikely that any improvement in the intrinsic performance of the detector will significantly impact on system performance.

Single photon development continues strongly. Increasingly attenuation correction systems that use transmission sources will be used clinically. Multi-detector cameras continue to be popular as a way of improving camera sensitivity. Reconstruction techniques are becoming increasingly complex, facilitated by increasing computer power. Analysis of results, especially in the area of gated myocardial perfusion imaging has also benefited from this power.

Many departments are now integrated into hospital wide area networks and "intranets" that allow images, and not just study reports, to be available to referring personnel.

Acknowledgements

I would like to thank Ms. Ailsa Cowie for extensive manuscript revision. Thanks also to Dale Bailey of the MRC Cyclotron Unit in Hammersmith UK for his illustration used in Figure 11.

REFERENCES

1. Links JM. Advances in nuclear medicine instrumentation: considerations in the design and selection of an imaging system. *Eur J Nucl Med.* 1998; 25:1453–1466.

2. Rich DA. A brief history of positron emission tomography. *J Nuc Med Tech.* 1997; 25:4–11.

3. Moses WW, Derenzo SE. Scintillators for positron emission tomography. Proceedings of the Scint'95, pp.9–16, (Edited by Dorenbos P and Eijk CW;, Delft, The Netherlands, 1996.

4. New Equipment in Nuclear Medicine, Part 1: Solid-State Detectors. *J Nucl Med.* 1998; 39(11):15N.

5. Hudson HM, Larkin RS. Accelerated image reconstruction using ordered subsets of projection data. *IEEE Trans Med Imaging.* 1994; 13:601–609.

6. Hutton BF, Hudson HM, Beekman FJ. A clinical perspective of accelerated statistical reconstruction. *ANZSNM Newsletter.* 1997; 28(4):16–29.

7. Heller SL, Goodwin PN. SPECT instrumentation: Performance, lesion detection, and recent innovations. *Seminars in Nucl Med.* 1987;XVII:184–199.

8. Blend MJ, Bhupendra AP, Rubas D, et al. Foil collimator defects: A comparison with cast collimators. *J Nuc Med Tech.* 1992;20:18–22.

9. Tsui BMW, Gullberg GT, Edggerton ER. Design and clinical utility of a fan beam collimator for SPECT imaging of the head. *J Nucl Med.* 1986;27(6):810–819.

10. Jaszczak RJ, Greer KL, Coleman RE. SPECT using a specially designed cone beam collimator. *J Nucl Med.* 1988; 29:1398–1405.

11. Smart R, Changes in installed gamma cameras in Australia. *ANZSNM Newsletter* 1996; 27 number 3:26.

12. Fleming JS. A technique for using CT images in attenuation correction and quantification in SPECT. *Nucl Med Comm.* 1989; 10:83–97.

13. Gullberg GT. Innovative design concepts for transmission CT in attenuation corrected SPECT imaging. *J Nucl Med.* 1998;Editorial;39:1344–1347.

14. Bailey DL, Hutton BF, Walker PJ. Improved SPECT using simultaneous emission and transmision tomography. *J Nucl Med.* 1987; 28:844–851.

15. Beekman FJ, Kamphuis C, Hutton BF, et al. Half-fanbeam collimators combined with scanning point sources for simultaneous emission-transmission imaging. *J Nucl Med.* 1998;39:1996–2003.

16. Derenzo SE, Moses WW, Huesman RH. Critical instrumentation issues for < 2mm resolution, high sensitivity brain PET. In "Quantification of brain function". Edited by Uemura K, Lassen NA, Jones T, et al. Elsevier Science Publishers, Amsterdam, Netherlands, 1993:25–37.

17. Chatziioannou AF, Cherry SR, Shao Y, et al. Performance evaluation of microPET: A high-resolution Lutetium Oxyorthosilicate PET scanner for animal imaging. *J Nucl Med.* 1999;40:1164–1175.

18. Budinger TF. PET instrumentation: What are the limits? *Semin Nucl Med.* 1998; XXVIII:247–267.

19. Huber JS, Moses WW, Derenzo SE, et al. Characterization of a 64 channel PET detector using photodiodes for crystal identification. *IEEE Trans Nuc Sci.* 1997; 44:1197–1201.

20. Bailey DL, Young H, Bloomfield PM, et al. ECAT ART – a continuously rotating PET camera: performance characteristics, initial clinical studies, and installation considerations in a nuclear medicine department. *Eur J Nucl Med.* 1997; 24:6–15.

21. Bailey DL. Transmission scanning in emission tomography. *Eur J Nucl Med.* 1998;25:774–787.

22. Carson RE, Daube-Witherspoon ME, Green MV. A method for postinjection PET transmission measurements with a rotating source. *J Nucl Med.* 1988;29:1558–1567.

23. Benard F, Smith R, Hustinx R. Clinical evaluation of processing techniques for attenuation correction with Cs-137 in whole-body PET imaging. *J Nucl Med.* 1999;40:1257-1263.

24. Watson CC, Newport D, Casey ME. Evaluation of simulation-based scatter correction for 3D PET cardiac imaging. *IEEE Trans Nuc Sci* 1997;44(3):90–97.

25. Karp JS, Muehllehner G, Mankoff DA. Continuous-slice PENN-PET: A positron tomograph with volume imaging capability. *J Nucl Med.* 1990;31:617–627.

26. Karp JS, Freifelder R, Geagan MJ. Three-dimensional imaging characteristics of the HEAD PENN-PET scanner. *J Nucl Med.* 1997;38:636–643.

27. Riggins SL, Kilroy KJ, Smith RJ. Clinical PET imaging with the C-PET camera. *J Nucl Med. Tech.* 2000;28:23–28.

28. Beyer T, Townsend DW, Brun T, et al. A combined PET/CT scanner for clinical oncology. *J Nucl Med.* 2000;41:1369–1379.

29. Kunze WD, Baehre M, Richter E. PET with dual-head coincidence camera: Spatial resolution, scatter fraction, and sensitivity. *J Nucl Med.* 2000;41:1067–1074.

30. Weber WA, Neverve J, Sklarek J. Imaging of lung cancer with flourine-18 FDG: comparison of a dual-head gamma camera in coincidence mode with a full-ring PET. *EJNM* 1999; 26:388–395.

31. Boren EL, Delbeke D, Patton J, et al. Comparison of FDG PET and coincidence detection imaging using a dual-head gamma camera with 5/8-inch NaI(Tl) crystals in patients with suspected body malignancies. *Eur J Nucl Med.* 1999;26:379–387.

32. Shreve P, Stevenson RS, Deters EC, et al. Oncologic diagnosis with 2-[Fluorine-18] Fluoro-2-deoxy-D-glucose imaging dual-head coincidence gamma camera versus positron emission tomographic scanner. Radiology 1998;207:431–437.

33. Muehllehner G, Geagan M, Countryman P. SPECT scanner with PET coincidence capability [abstract]. *J Nucl Med.* 1995;36:70P.

34. Melcher CL. Scintillation crystals for PET. *J Nucl Med.* 2000;41:1051–1055.

35. Derenzo SE, Weber MJ, Moses WW, et al. Methods for a systematic, comprehensive search for fast, heavy scintillator materials. Proceedings of the Material Research Society: Scintillator and Phosphor materials, 348:39–49 (Editor Weber MJ), San Francisco, Calif. 1994.

36. Newiger H, Hamisch P, Oehr J, et al. Physical Principles. In: PET in Oncology – Basics and clinical applications. (Eds. Ruhlmann J, Oehr P, Biersack H-J); Springer-Verlag, Berlin-Heidelberg, 1999:3–33.

37. Townsend DW, Isoardi RA, Bendriem B. Volume imaging tomographs. In *The Theory and Practice of 3D PET*. (Eds. Bendriem B, Townsend DW); Kluwer Academic; Amsterdam,The Netherlands: 1998:111–132.

38. Eberl S, Zimmerman RE. Nuclear medicine imaging and instrumentation. In *Nuclear Medicine in Clinical Diagnosis and Treatment.* 2nd Ed. (Eds. Murray IPC, Ell PJ); Churchhill Livingstone; Edinburgh: 1998:1559–1569.

39. Meikle SR, Dahlbom M. Positron emission tomography. In *Nuclear Medicine in Clinical Diagnosis and Treatment.* 2nd Ed. (Eds. Murray IPC, Ell PJ); Churchhill Livingstone; Edinburgh: 1998:1603–1616.

40. Moses WW, Derenzo SE. Prospects for time-of-flight PET using LSO scintillator. *IEEE Trans Nucl Sci*. 1999;46:474–478.

QUESTIONS

1. Which one of the following statements is **incorrect**?

   a. The basic design of the NaI detector has remained unchanged for the last 10 years.
   b. Increased computing power is allowing more complex reconstruction and analysis in nuclear medicine and PET.
   c. Measured attenuation correction is gaining clinical acceptance in nuclear medicine.
   d. Multiheaded gamma cameras were introduced to reduce radio-pharmaceutical costs.

2. Photons lose a portion of their energy when they undergo Compton scatter. Which one of the following options is correct? Scattered photons are rejected during acquisition by which of the following processes?

   a. Timing delay
   b. Energy window discrimination
   c. The Doppler effect
   d. Coincidence windowing

3. Which of the following physical properties of scintillation detectors effects energy resolution most?

   a. High stopping power
   b. High photon yield
   c. Refractive index
   d. Density

4. A photon with energy of 140keV undergoes Compton scatter and its direction is changed by 35 degrees. The photon's post collision energy will be:

   a. 103 keV
   b. 113 keV
   c. 123 keV
   d. 133 keV

5. Typically, only around 1 in 10000 photons from the patient will reach the gamma camera detector. Which one of the following best explains this inefficiency?

   a. Only a small section of the patient is in the field of view of the detector.
   b. Attenuation of photons by the body.
   c. Decay of the isotope between administration and imaging.
   d. Attenuation by the collimator.

6. When comparing the system sensitivity of PET and SPECT which one of the following is correct?

   a. PET has greater sensitivity because it doesn't need collimation.
   b. PET has greater sensitivity purely because for each decay 2 photons are emitted.
   c. PET has greater sensitivity because the higher photon energy means less attenuation.
   d. PET has greater sensitivity because it has 360 degrees of detectors around the patient.

7. A gamma camera has detector (intrinsic) resolution of 4.0 mm and collimator resolution of 10.0mm. If detector resolution was reduced to 2.0mm, then system resolution would change from:

   a. 14 mm to 12 mm
   b. 40 mm to 20 mm
   c. 12.2 mm to 11.8 mm
   d. 10.8 mm to 10.2 mm

8. Sodium Iodide NaI(Tl) has virtually been the exclusive choice for scintillation detectors in gamma cameras for 30 years. Which of the following is **incorrect**?

   a. NaI(Tl) has excellent stopping power which gives it high sensitivity to medium and high energy photons.
   b. NaI(Tl) has a good light photon yield which gives it good energy resolution.
   c. Despite being hygroscopic, it can be manufactured relatively cheaply.
   d. NaI(Tl) has a good light photon yield which allows it to be manufactured into a large crystal and coupled to multiple PMTs.

9. Which one of the following statements relating to BGO PET detectors is **incorrect**?

    a. BGO has relatively poor energy resolution.
    b. BGO has excellent photon stopping power.
    c. BGO is manufactured into block detectors rather than large single detectors.
    d. BGO is a likely replacement for NaI as a gamma camera detector.

10. Despite having many superior physical properties to NaI, LSO is unlikely to become a material of choice in SPECT gamma cameras. Which one of the following explanations is **incorrect**?

    a. NaI has better stopping power.
    b. LSO is very expensive.
    c. The effect of collimation on extrinsic resolution dilutes any improvement in intrinsic resolution.
    d. LSO is inherently radioactive.

11. Select the correct statement. Semiconductor detectors:

    a. Have worse energy resolution than scintillator/PMT type detectors.
    b. Will be much heavier and larger than scintillator/PMT type detectors of a comparable FOV.
    c. Are constructed in a matrix of individual detectors, with each cell being the minimum resolvable unit.
    d. Are used in most current gamma cameras.

12. Which statement relating to filtered back projection tomographic reconstruction is **incorrect**?

    a. Can produce serious artifacts in low count studies, in particular, 'starring' of counts from 'hot' structures.
    b. The 'Ramp' filter corrects for the blurring effect caused by statistical noise.
    c. Has only limited capability of correcting for attenuation and scatter.
    d. It is the most commonly used reconstructive algorithm, even today.

13. Which statement relating to iterative tomographic reconstruction is **incorrect**?

    a. It has become increasingly utilized with the availability of faster computing.
    b. Iterative techniques achieve reconstruction by comparing acquired data to what has been reconstructed in the previous iteration. The reconstructed data is modified to minimize any difference.
    c. Iterative reconstruction should only be used in 'high count' studies.
    d. The OSEM iterative technique is able to achieve reconstruction at an accelerated rate compared to conventional iterative reconstruction.

14. What is the sensitivity of a collimator (with hexagonal holes) with the following properties _____?

    Hole length (L) = 35 mm
    Septal thickness (s) = 0.2 mm
    Hole diameter (d) = 2.2 mm

    a. One photon per 4
    b. One photon per 43
    c. One photon per 436
    d. One photon per 4365

15. Using the collimator properties defined in Question 7, what would be its resolution at a scanning depth of 100mm?

    a. 7.5 mm
    b. 8.5 mm
    c. 9.5 mm
    d. 10.5 mm

16. Which one of the following statements regarding fan-beam collimators is **incorrect**?

    a. SPECT studies can be reconstructed with the same algorithm used for parallel hole collimators.
    b. They are parallel in the axial plane.
    c. They are convergent in the transaxial plane.
    d. Their FOV is smaller than parallel hole collimators and therefore are only suitable for neurology and pediatric SPECT.

17. Which one of the following statements regarding cone-beam collimators is **incorrect**?

    a. The holes in cone-beam collimators all converge to a focal point.
    b. Reconstruction of SPECT studies is complex due to the data having been acquired obliquely through transaxial planes.
    c. Increased sensitivity is due to the focused geometry of the collimator.
    d. The collimator is suitable for all SPECT studies.

18. Multi-detector gamma cameras have some advantages over single detector systems. Which of the following statements is false?

    a. Multi-detector gamma cameras can reduce acquisition times.
    b. Multi-detector gamma cameras can improve resolution.
    c. Multi-detector gamma cameras can reduce attenuation.
    d. Multi-detector gamma cameras can improve sensitivity.

19. Which of the following statements pertaining to SPECT attenuation correction is false?

    a. First order attenuation correction assumes homogeneous attenuation within the body and therefore achieves good correction of myocardial studies.
    b. A transmission source should be selected with a photon whose energy is similar to that of the emission photon so that accurate determination of attenuation coefficients can be achieved.
    c. A transmission source should be well shielded when in use.
    d. Moving transmission sources, either as point or line sources, allow regional concentration of photons, thus reducing the percentage of contamination from emission photons.

20. Which one of the following does not effect the resolution of a PET scanner:

    a. Positron range
    b. Uptake time
    c. Annihilation photon non-colinearity
    d. Detector element size

21. Which of the following statements is **incorrect**? “Positron range”:

    a. Is the distance a PET camera needs to be to a cyclotron to make if economically viable.
    b. Is the average distance a positron travels from the nucleus before it annihilates with an electron.
    c. Degrades PET resolution.
    d. Is related to the E_{max} of the isotope used.

22. Which of the following statements is **incorrect**? In PET scanning, “Annihilation photon non-colinearity”:

    a. Results in reduced sensitivity.
    b. Degrades PET resolution by about 2 mm in a human scanner.
    c. Is caused by the annihilation photons not traveling in exactly opposite directions.
    d. Has greatest effect when the diameter of PET detectors is increases.

23. Which one of the following statements is correct? In PET scanning, “Depth of Interaction” analysis:

    a. Is the calculation of the point within the patient where radioactive decay occurs.
    b. Is used to determine coincidence timing in ‘time-of-flight’ scanners.
    c. Helps to correct for detector parallax errors in coincidences occurring away from the center of the FOV.
    d. Determines the position of a rotating transmission source.

24. Which one of the following scintillation detector materials has the best stopping power for 511 keV photons?

    a. NaI(Tl)
    b. BGO
    c. LSO
    d. GSO

25. Which one of the following scintillation detector materials has the best photon yield?

    a. NaI(Tl)
    b. BGO
    c. LSO
    d. GSO

26. Which one of the following scintillation detector materials has the best photon decay constant for PET?

    a. NaI(Tl)
    b. BGO
    c. LSO
    d. GSO

27. Which combination of properties below would you select as belonging to an ideal PET detector?

    a. high stopping power, low photon yield and long photon decay constant.
    b. high stopping power, high photon yield and long photon decay constant.
    c. low stopping power, high photon yield and short photon decay constant.
    d. high stopping power, high photon yield and short photon decay constant.

28. Using the combined properties selected in the questions 27, which of the following materials would make the best PET detector?

    a. NaI(Tl)
    b. BGO
    c. LSO
    d. YSO
    e. BaF2

29. Which of the following statements is **incorrect**? When acquiring PET studies in 3D mode

    a. There is an increased scatter fraction when compared to 2D acquisitions.
    b. Sensitivity increases towards the center of the axial FOV.
    c. The detectors are not shielded from out-of-field activity.
    d. There is approximately a 5 fold decrease in sensitivity compared to 2D acquisitions.

30. Which one of the following statements concerning attenuation in PET is **incorrect**?

    a. Attenuation of 511keV photons by soft tissue negligible and therefore correction only needs to be performed in large patients.
    b. The attenuation effect in PET is considerable despite the use of 511keV photons due to both annihilation photons needing to be detected to form a coincidence.
    c. The effect of attenuation in PET is approximately equivalent to that suffered by 201Tl imaging using SPECT.
    d. The effects of attenuation is greatest towards the middle of the body.

31. Select the **one incorrect statement**. Post-injection PET attenuation correction:

    a. Allows the transmission scan to be acquired after the patient has been injected.
    b. Are achieved by differentiating between photons arising from the patient and the transmission source.
    c. Improves throughput of the scanner.
    d. Can only be performed before the emission study.

32. Select the **one incorrect statement** below. Singles PET attenuation correction:

    a. Allows a transmission source of increased activity to be employed thus reducing acquisition time.
    b. Separation of emission and transmission gamma rays is achieved by energy discrimination.
    c. Longer half-life sources can be utilized thus reducing frequency and cost of replacement.
    d. Cannot be acquired once a patient has been administered activity.

33. Select the **one correct answer** below. Image segmentation of transmission data:

    a. Allows for more accurate calculation of attenuation coefficients.
    b. Removes noise from areas of equivalent attenuation in the transmission image by applying a uniform attenuation coefficient value.
    c. Corrects for subtle differences in attenuation coefficients in the patient.
    d. Corrects for the effects of scatter contribution.

34. Which of the following statements relating to the Penn-PET scanner with Sodium Iodide detectors is **incorrect**?

    a. Detector dead time is reduced by logically dividing each detector into a number of smaller "virtual" detectors.
    b. Detector dead time is reduced by using only a central PMT and the surrounding 6 PMTs to determine the position of a scintillation event.
    c. Detector dead time is reduced by clipping the output signal from individual PMTs after a finite period of time.
    d. Detector dead time is reduced by using large integral detectors.

35. Which one of the following statements is **incorrect** concerning "Partial ring BGO PET scanners"?

    a. The scanner only operates in 3D acquisition mode.
    b. The scanner has twice the sensitivity of a full ring BGO PET scanner.
    c. Manufacturing costs are reduced by using approximately half the number of detectors arranged in two opposing banks.
    d. Manufacturing costs are reduced by using detectors with reduced depth.

36. Which one of the following statements is **incorrect** concerning Hybrid PET/SPECT gamma cameras?

    a. The high count-rates experienced when imaging in PET mode can be negated by installing collimators.
    b. Increasing crystal thickness to improve sensitivity to 511 keV photons reduces intrinsic resolution.
    c. Open detector geometry results in a large contribution from out-of-field activity.
    d. The camera has relatively poor sensitivity due to partial geometry and the use of detectors whose thickness is not optimal for 511 keV.

37. Which one of the following statements is **incorrect** concerning Hybrid PET/SPECT gamma cameras?

    a. They are not suitable for short half-life isotope studies because of the very high transient count-rates experienced.
    b. They are economically attractive due to small capital cost compared to dedicated PET cameras.
    c. They are economically attractive as they can be used as a gamma camera when isotope may not be available.
    d. They have equivalent performance characteristics compared to dedicated PET cameras.

38. When selecting a scintillation detector material for "time-of-flight" PET scanning the most important physical property is:

    a. Cost
    b. Density
    c. Light photon decay constant
    d. Stopping power

39. Which of the following statements regarding combined PET/CT scanners is **incorrect**?

    a. Attenuation correction of the PET emission data can be calculated from the CT data.
    b. Improved diagnostic accuracy may be achieved by precise co-registration of structure (CT) and function (PET).
    c. Patients being scanned will need to hold their breath between scans.
    d. PET and CT scans are acquired at separate times in the one session.

40. The use of slotted NaI(Tl) detectors improve efficiency in PET mode and resolution in SPECT mode of hybrid gamma cameras. Which statement below best describes how this is achieved?

    a. The slots in the crystal stop 511keV photons scattering throughout the crystal.
    b. The slots allow gamma photons traveling perpendicular to the detector surface to reach the rear of the crystal.
    c. Resolution is maintained in a thicker crystal by reducing the radial spread of light photons within the crystal via the use of slots.
    d. Higher sensitivity in PET mode is achieved by the crystal having variable thickness.